The Astrophysical Journal, 609:935–951, 2004 July 10

GAMMA-RAY BURST FORMATION RATE INFERRED FROM THE SPECTRAL PEAK ENERGY–PEAK LUMINOSITY RELATION

D. Yonetoku,[1] T. Murakami,[1] T. Nakamura,[2] R. Yamazaki,[2] A. K. Inoue,[2] and K. Ioka[3]

Received 2003 September 2; accepted 2004 March 24

ABSTRACT

We estimate a gamma-ray burst (GRB) formation rate based on the new relation between the spectral peak energy (E_p) and the peak luminosity. The new relation is derived by combining the data of E_p and the peak luminosities by *BeppoSAX* and BATSE, and it looks considerably tighter and more reliable than the relations suggested by the previous works. Using the new E_p-luminosity relation, we estimate redshifts of the 689 GRBs without known distances in the BATSE catalog and derive a GRB formation rate as a function of the redshift. For the redshift range of $0 \leq z \leq 2$, the GRB formation rate increases and is well correlated with the star formation rate, while it keeps constant toward $z \sim 12$. We also discuss the luminosity function and the redshift dependence of the intrinsic luminosity (luminosity evolution).

Subject headings: early universe — gamma rays: bursts

On-line material: machine-readable table

1. INTRODUCTION

Many ground-based telescopes observed optical afterglows of gamma-ray bursts (GRBs) and measured their redshifts by detecting the absorption and/or emission lines of the interstellar matter in the host galaxy. However, the number of GRBs with measured redshift is only a fraction of all GRBs detected with BATSE and the *BeppoSAX*, *HETE-2*, and *INTEGRAL* satellites. We still have only about 30 GRBs with known redshifts (Frail et al. 2001; Bloom et al. 2003). Most of them occur at cosmological distances, and the current record holder is GRB 000131 at $z = 4.5$ (Andersen et al. 2000). According to the brightness distribution of GRBs with known redshifts, we should have already detected much more distant GRBs, such as at $z \sim 20$ (Band 2003). If we can establish a method for estimating the intrinsic brightness in the characteristics of prompt gamma-ray emission, we can use the GRB brightness as a standard candle to determine the redshifts of a majority of GRBs, which would enable us to explore the early universe out to $z \sim 20$.

Using geometrical corrections of collimated jets, Frail et al. (2001) and Bloom et al. (2003) revealed that the bolometric energies released in prompt emission cluster tightly around the standard energy of $\sim 1 \times 10^{51}$ ergs. Thus, the explosion energy of GRBs can be used as a standard candle, like the supernovae. However, the apparent brightness of GRBs strongly depends on the jet opening angle and the viewing direction. To use GRB brightness as a standard candle, we need to correct for such effects.

Several authors have tried to establish a method for estimating isotropic luminosity from observed GRB properties. Using the variability-luminosity relation of prompt gamma-ray emissions, Fenimore & Ramirez-Ruiz (2000) have done pioneering work based on the fact that variable GRBs are much brighter than the smoother ones. Spectral time lag, which is the interval between the pulse arrival times of two different energy bands, also correlates with the isotropic luminosity (Norris et al. 2000). These properties might be due to the effect of the viewing angle to the GRB jet (e.g., Ioka & Nakamura 2001; Norris 2002; Murakami et al. 2003). More recently, based on a spectral analyses of the *BeppoSAX* data alone, Amati et al. (2002) found a correlation between the total energies radiated in GRBs and the peak energies E_p, which are the energies at the peak of νF_ν spectrum. Atteia (2003) suggested the possibility of using this as an empirical redshift indicator.

Applying these luminosity indicators to GRBs without known redshifts, previous works have estimated GRB redshifts from the apparent gamma-ray brightness. Several authors (e.g., Fenimore & Ramirez-Ruiz 2000; Norris et al. 2000; Schaefer et al. 2001; Lloyd-Ronning et al. 2002a; Murakami et al. 2003) have discussed GRB formation rates as the results of the derived redshift distributions. Especially, using a mathematically rigid method (Efron & Petrosian 1992; Petrosian 1993; Maloney & Petrosian 1999), Lloyd-Ronning et al. (2002a) have estimated the GRB formation rate from the variability-luminosity relation. These works gave basically the same results. GRB formation rates increase with redshift at $0 \lesssim z \lesssim 2$ and keep on rising up to the higher redshift of $z \sim 12$. The GRB formation rates did not decrease with z, in contrast with the star formation rates (SFRs) measured in the UV, optical, and infrared bands (e.g., Madau et al. 1996; Lilly et al. 1996; Barger et al. 2000; Stanway et al. 2003). However, the empirical relations used in previous works have not been very reliable and are sometimes still in debate.

In this paper we use a new and much tighter relation, based on the E_p-luminosity relation of prompt gamma-ray emission, to estimate the redshifts, combining not only *BeppoSAX* data but also 11 BATSE GRBs with known redshifts. Importantly, the correlation is higher and the uncertainty of our relation is much less than those of previous works using lags and variability. Applying the new relation, we estimate the redshifts of 689 GRBs and then demonstrate the GRB formation rate out to $z \sim 12$ for a flux-limited sample (Efron & Petrosian 1992;

[1] Department of Physics, Faculty of Science, Kanazawa University, Kakuma, Kanazawa, Ishikawa 920–1192, Japan; yonetoku@astro.s.kanazawa-u.ac.jp.
[2] Department of Physics, Kyoto University, Kyoto 606-8502, Japan.
[3] Department of Earth and Space Science, Osaka University, Toyonaka, Osaka 560-0433, Japan.

TABLE 1
SPECTRAL PARAMETERS FOR 11 KNOWN-REDSHIFT GRBS OF BATSE

GRB	Redshift	α	β	$E_p(1+z)$ (keV)	Peak Flux (10^{-6} ergs cm^{-2} s^{-1})	Peak Luminosity 10^{52} ergs s^{-1}	χ^2/dof	k_c
970508.....	0.835	$-1.03^{+1.51}_{-0.06}$	$-2.20^{+0.10}_{-0.11}$	$89.8^{+37.8}_{-29.7}$	0.45 ± 0.10	0.14 ± 0.01	43.8/40	1.6
970828.....	0.9578	$-0.45^{+0.06}_{-0.06}$	$-2.06^{+0.08}_{-0.10}$	$742.6^{+29.4}_{-32.1}$	5.93 ± 0.34	3.67 ± 0.15	96.0/82	1.5
971214.....	3.418	$-0.36^{+0.14}_{-0.14}$	$-3.10^{+0.52}_{-6.90}$	$806.7^{+48.6}_{-63.2}$	1.25 ± 0.28	19.51 ± 0.17	68.9/66	1.2
980326.....	0.9–1.1	$-0.93^{+0.09}_{-0.08}$	$-2.96^{+0.21}_{-0.51}$	35.0–100.0	0.65 ± 0.15	0.24–0.40	55.7/48	1.4
980329.....	2.0–3.9	$-0.79^{+0.03}_{-0.03}$	$-2.27^{+0.04}_{-0.05}$	785.0–1085.0	5.79 ± 4.17	12.49–72.38	121.1/112	1.3
980703.....	0.966	$-0.80^{+0.22}_{-0.16}$	$-1.60^{+0.06}_{-0.09}$	>150.0	2.64 ± 0.51	1.76 ± 0.05	89.6/91	1.3
990123.....	1.600	$-0.18^{+0.08}_{-0.07}$	$-2.33^{+0.08}_{-0.09}$	$1333.7^{+49.8}_{-56.9}$	19.6 ± 0.16	31.22 ± 0.23	134.1/112	1.2
990506.....	1.30	$-0.90^{+0.19}_{-0.13}$	$-2.08^{+0.08}_{-0.10}$	$737.6^{+69.2}_{-87.8}$	9.36 ± 0.20	13.28 ± 0.10	108.3/103	1.3
990510.....	1.619	$-0.71^{+0.12}_{-0.12}$	$-3.79^{+0.51}_{-6.21}$	$538.4^{+22.3}_{-32.1}$	2.98 ± 0.18	6.19 ± 0.06	89.9/111	1.4
991216.....	1.020	$-0.66^{+0.04}_{-0.04}$	$-2.44^{+0.12}_{-0.17}$	$1083.7^{+37.3}_{-41.3}$	61.4 ± 1.21	32.36 ± 0.11	125.8/102	1.2
000131.....	4.5	$-0.91^{+0.20}_{-0.15}$	$-2.02^{+0.18}_{-0.32}$	$926.0^{+97.5}_{-83.1}$	2.67 ± 0.41	51.35 ± 7.88	115.1/97	1.4

Petrosian 1993; Maloney & Petrosian 1999; Lloyd-Ronning et al. 2002a). The present work is the first to derive the GRB formation rate on the basis of the E_p-luminosity relation. Throughout the paper, we assume a flat-isotropic universe with $\Omega_m = 0.32$, $\Omega_\Lambda = 0.68$, and $H_0 = 72$ km s^{-1} Mpc^{-1} (Bennett et al. 2003; Spergel et al. 2003).

2. DATA ANALYSIS

First, we analyzed 11 GRBs in the BATSE archive with known redshifts (970508, 970828, 971214, 980326, 980329, 980703, 990123, 990506, 990510, 991216, and 000131). Following previous work by Amati et al. (2002), we calculate the E_p of the burst average spectra and the peak luminosity integrating between 1 s intervals at the peak, because this is a better distance indicator than the burst average luminosity.

We used spectral data detected by the BATSE LAD detectors and performed a spectral analysis with the standard data reduction for each GRB.[4] We extracted the burst data in the $\sim T_{90}$ interval for each burst and subtracted the background spectrum derived from the average spectrum before and after the GRB in the same data set. We adopted the spectral model of a smoothly broken power law (Band et al. 1993). The model function is described below:

$$N(E) = \begin{cases} A\left(\dfrac{E}{100\ \mathrm{keV}}\right)^{\alpha} \exp\left(-\dfrac{E}{E_0}\right), & \text{for } E \le (\alpha-\beta)E_0, \\ A\left(\dfrac{E}{100\ \mathrm{keV}}\right)^{\beta} \left[\dfrac{(\alpha-\beta)E_0}{100\ \mathrm{keV}}\right]^{\alpha-\beta} \exp(\beta-\alpha), & \text{for } E \ge (\alpha-\beta)E_0. \end{cases} \quad (1)$$

Here $N(E)$ is in units of photons cm^{-2} s^{-1} keV^{-1} and E_0 is the energy at the spectral break; α and β are the low- and high-energy power-law indices, respectively. For the cases of $\beta < -2$ and $\alpha > -2$, the peak energy can be derived as $E_p = (2+\alpha)E_0$, which corresponds to the energy at the maximum flux in the νF_ν spectra. The peak luminosity with the proper k-correction can be calculated as $L = 4\pi d_L^2 F_\gamma k_c$, where d_L and F_γ are the luminosity distance and observed peak flux integrated between 30 and 10,000 keV, respectively. The k-correction factors (k_c) are estimated by the same method used by Amati et al. (2002), are consistent with the ones of Bloom et al. (2001), and do not exceed 2. We summarize the fitting results for the 11 GRBs in Table 1.

[4] See http://cossc.gsfc.nasa.gov/analysis/index.html.

3. E_P-LUMINOSITY RELATION

In Figure 1 we show the peak luminosities, in units of 10^{52} ergs s^{-1}, as a function of peak energy, $E_p(1+z)$, in the rest frame of each GRB. For GRB 980703, only a lower limit of $E_p(1+z)$ is set because of the spectral index $\beta > -2$. The *BeppoSAX* results reported by Amati et al. (2002) are also included in the same figure after correcting the energy range. Here we converted the peak fluxes of Amati et al. (2002, their Table 1) into the peak luminosity of our energy range of 30–10,000 keV, using their spectral parameters. Therefore, we can combine our 11 BATSE results with *BeppoSAX* results in the same plane. This is the key to the present work.

There is a higher and tighter positive correlation between $E_p(1+z)$ and L than in previous works. The linear correlation coefficient, including the weighting factors, is 0.958 for 14 degrees of freedom (16 samples with firm redshifts[5];

[5] Since there are four samples detected by both *BeppoSAX* and BATSE, so the independent sample is 12.

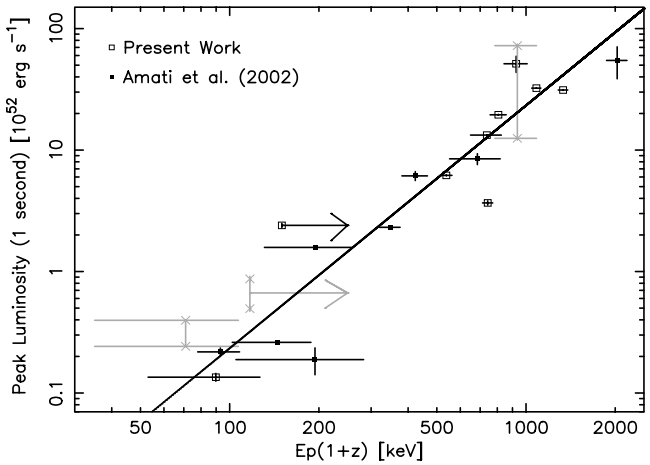

FIG. 1.—E_p-luminosity relation. The open squares are our present results with BATSE. The results of *BeppoSAX* (Amati et al. 2002) are also shown as the filled squares. Both results are plotted as $E_p(1+z)$ at the rest frame of the GRBs and the peak luminosity between 30 and 10,000 keV derived by the 1 s peak flux. The points shown with two crosses indicate the results of GRBs with ambiguous redshifts (GRB 980326, GRB 980329 and GRB 000214). The solid line is the best-fit power-law model for the data.

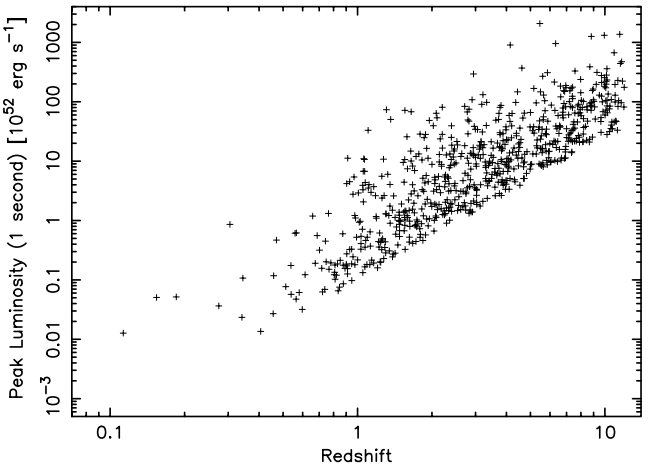

FIG. 2.—Distribution of the peak luminosity vs. redshift derived from the E_p-luminosity relation. The truncation of the lower end of the luminosity is caused by the flux limit of $F_{\rm limit} = 2 \times 10^{-7}$ ergs cm^{-2} s^{-1}.

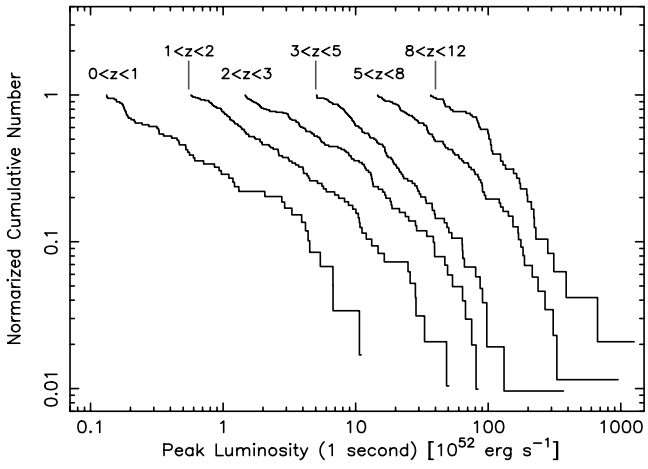

FIG. 3.—Cumulative luminosity function normalized to unity for the purpose of easy comparison of those shapes, in the several redshift ranges. The shape of the luminosity functions looks like a broken rather than a single power-law shape. Moreover, luminosity evolution may exist because the break luminosities increase toward the higher redshift.

Fig. 1, *open and filled squares*) for $\log [E_p(1+z)]$ and $\log [L]$. The chance probability shows an extremely low value of 5.31×10^{-9}. When we adopt the power-law model to the E_p-luminosity relation, the best-fit function is

$$\frac{L}{10^{52}\ \mathrm{ergs\ s^{-1}}} = (2.34^{+2.29}_{-1.76}) \times 10^{-5} \left[\frac{E_p(1+z)}{1\ \mathrm{keV}} \right]^{2.0 \mp 0.2}, \quad (2)$$

where the uncertainties have a 1 σ error.

4. REDSHIFT ESTIMATION AND GRB FORMATION RATE

The E_p-luminosity relation derived from *BeppoSAX* and BATSE in the previous section seems to be a much better indicator of the peak luminosity than the spectral time lag and variability of GRBs (Norris et al. 2000; Fenimore & Ramirez-Ruiz 2000; Schaefer et al. 2001), since the correlation is higher. In this section, using the E_p-luminosity relation, we try to estimate the peak luminosities and the redshifts of the BATSE GRBs without known redshifts.

First, we picked up about 1000 brighter GRBs from the BATSE triggered event list in a class of with the long duration of $T_{90} > 2$ s. Then, we extracted the average spectrum for each GRB. We excluded GRBs that did not have full data of T_{90} duration and/or the appropriate detector response matrices.[6] For the other good samples, we performed spectral analysis using the method described in § 2. After setting the flux limit of $F_{\rm limit} = 2 \times 10^{-7}$ ergs cm^{-2} s^{-1} in order to have a better signal-to-nosie ratio, 745 samples remained in this selection. Having obtained the 1 s peak flux F_γ and E_p at the observer's rest frame, we can estimate the redshift using equation (2). The estimated redshifts of 21 samples are beyond $z > 12$, and 35 have no solution satisfying equation (2). For example, 12 GRBs in the 220 samples of Fenimore & Ramirez-Ruiz (2000) (trigger numbers: 678, 1468, 1601, 1623, 2193, 2383, 2428, 2890, 2984, 2993, 3593, and 5473) have no solution, and seven (2780, 3040, 3405, 3860, 5450, 5484, and 5526) are beyond $z > 12$. These samples show large $E_p \sim 1000$ keV at the observer's rest frame, but their peak luminosities are quite dim. In this case, the redshifts are extremely large and the solution cannot be obtained from our E_p-luminosity relation. Therefore, hereafter we treat 689 samples within the redshift range of $z \leq 12$ that were studied in previous works. The list of 689 samples, with the observed E_p, estimated redshift, and luminosity with 1 σ error, is summarized in Table 2.

In Figure 2 we show the distribution in the (z, L) plane truncated by the flux limit. The cumulative luminosity functions, normalized to unity, at each redshift interval are shown in Figure 3. These luminosity functions look like a broken rather than a single power law. These shapes are similar to each other, but the break luminosities seem to increase toward higher redshift. This fact indicates that the luminosity itself depends on the redshift, so the luminosity evolution is hidden in the (z, L) plane in Figure 2, but the form of the luminosity functions has remained constant.

4.1. *Luminosity Evolution*

For simplicity, it is better to separate the luminosity evolution from the stable form of the luminosity function. The total luminosity function $\Phi(L, z)$ can be rewritten as $\Phi(L, z) = \rho(z)\phi(L/g_k(z), \alpha_s)/g_k(z)$ without loss of generality. Here each function means the luminosity evolution $g_k(z)$, the GRB formation rate $\rho(z)$, and the local luminosity function $\phi(L/g_k(z), \alpha_s)$, respectively. Although the parameter α_s represents the shape of the luminosity function, we ignore the effect of this parameter because the shape of the luminosity function is approximately the same as shown in Figure 3. In this case, the GRB formation rate *only* as a function of z can be derived more simply. Therefore, we remove the effect of the luminosity evolution $g_k(z)$ from the (z, L) data set and then discuss the form of the cumulative luminosity function $\psi(L)$ and the GRB formation rate $\rho(z)$.

To estimate the luminosity evolution $g_k(z)$, we introduce a τ statistical method that has been used for quasar samples (Lynden-Bell 1971; Efron & Petrosian 1992; Petrosian 1993; Maloney & Petrosian 1999) and was first applied to GRB samples by Lloyd-Ronning et al. (2002a). When we notice the

[6] The data with the trigger number: 761, 1606, 1676, 1733, 1819, 2190, 2450, 2581, 2606, 2922, 3439, 3745, 3853, and 4368 in the 220 samples of Fenimore & Ramirez-Ruiz (2000) are excluded by this fact.

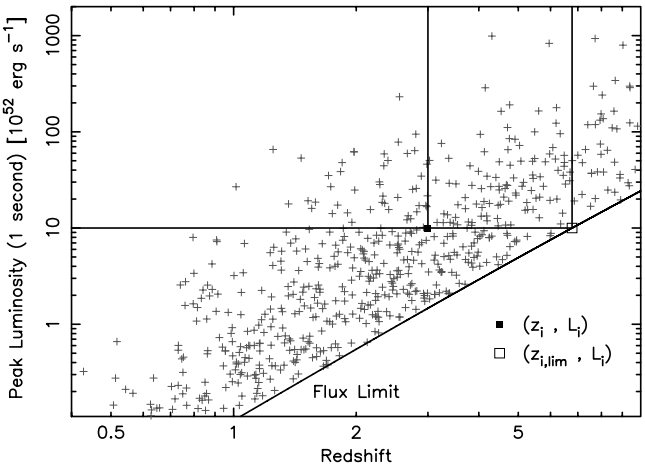

FIG. 4.—Example of the associated set. When we notice the ith sample of (z_i, L_i), the associated set can be determined as the region of both $L > L_i$ and $z < z_{i,\lim}$. The data in this set is free from the flux limit, so they can be considered equivalent to one other.

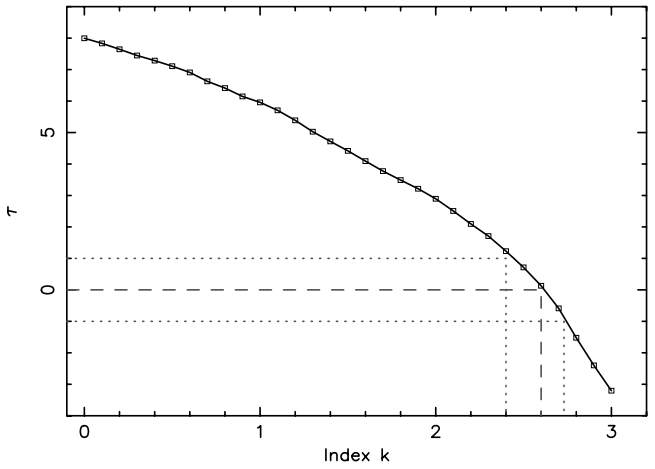

FIG. 5.—Determination of the parameter k of the luminosity evolution for the functional form of $g_k(z) = (1+z)^k$. The correlation statistic τ is shown as a function of k. The $\tau = 0$ is given at $k = 2.60^{+0.15}_{-0.20}$ with 1 σ statistical uncertainty, so $g_k(z) = (1+z)^{2.6}$ is the best function to describe the luminosity evolution. A hypothesis of no luminosity evolution (equivalent to $k = 0$) is rejected with 8.0 σ significance.

ith sample of (z_i, L_i), as shown in Figure 4, we can consider an associated set of

$$J_i = \{ j | L_j > L_i, z_j < z_{i,\lim} \}, \quad \text{for } 1 \le i \le 689, \tag{3}$$

defining the number of samples in the J_i set as N_i. Here, $z_{i,\lim}$ is the crossing point between two lines of the flux limit and $L = L_i$. When considering the region in J_i, we can regard them as equivalent, because the number distribution in the associated set is unrelated to the flux limit. If z_i and L_i are independent of each other, the number of sample,

$$R_i = \text{number}\{ j \in J_i | z_j \le z_i \}, \tag{4}$$

is uniformly distributed between 1 and N_i. Generally, to quantify the data correlation degree, the test statistic τ is introduced as

$$\tau = \frac{\sum_i (R_i - E_i)}{\sqrt{\sum_i V_i}}, \tag{5}$$

where $E_i = (N_i + 1)/2$ and $V_i = (N_i^2 - 1)/12$ are the expected mean and the variance for the uniform distribution, respectively. The summation is performed for all points of $1 \le i \le 689$. This τ value is similar to the Kendell's τ statistic, and it can be generalized to adopt to the flux-limited samples. If R_i is a completely uniform distribution, then the cases of $R_i \le E_i$ and $R_i \ge E_i$ appear to be equal, and we expect the τ value to be zero. Moreover, this τ value is normalized by the square root of variance, so the data correlation degree between z and L can be measured in units of standard deviation.

To separate the luminosity evolution $g_k(z)$, we assume the functional form $g_k(z) = (1+z)^k$, which is also used by Maloney & Petrosian (1999) and Lloyd-Ronning et al. (2002a). The value $L' \equiv L/g_k(z)$ corresponds to the luminosity after removing the luminosity-evolution effect. Using the τ statistic value for the (z, L') data, we calculate the data correlation degree. When τ shows a large value (large correlation degree), we change the index k and calculate the τ value again and again until finding the most proper index k giving $\tau = 0$. In Figure 5 we show the τ value as a function of the index k. The null hypothesis of the luminosity evolution is rejected at about the 8 σ confidence level ($\tau = 8.0$ at $k = 0$), and the best index is found to be $k = 2.60^{+0.15}_{-0.20}$ within 1 σ significance.

4.2. *Luminosity Function*

After converting the observed luminosity into $L' = L/(1+z)^{2.60}$ space, we can nonparametrically generate the cumulative luminosity function $\psi(L'_i)$ as a function of univariate L' with the following equation (Lynden-Bell 1971):

$$\ln \psi(L'_i) = \sum_{j<i} \ln\left(1 + \frac{1}{N_j}\right). \tag{6}$$

According to this equation, the cumulative number at the ith point is calculated from N_j, so there may be large ambiguities for cases of small N_j, such as, for example, $z \sim 0$. However, for our 689 samples, this uncertainty is not significant (i.e., $z = 0.5$, $z = 1.0$, and $z > 2.0$ have 30%, 10%, and less than 7% uncertainty, respectively).

In Figure 6 we show the luminosity functions of $L' = L/(1+z)^{2.60}$ after removing luminosity evolution. The shape of the luminosity function is a broken power law. The dimmer and the brighter ends of the functional form are represented by

$$\psi(L') \propto \begin{cases} L'^{-0.29 \pm 0.02} & \text{for } L'_{52} < 0.06, \\ L'^{-1.02 \pm 0.02} & \text{for } L'_{52} > 0.3, \end{cases} \tag{7}$$

with the break point at $L' \sim 1 \times 10^{51}$ ergs s^{-1}. This luminosity function corresponds to the *present* distribution at $z = 0$, because the effect of luminosity evolution is removed. Therefore, the luminosity function in the comoving frame is roughly estimated as $\psi(L')(1+z)^{2.60}$.

4.3. *GRB Formation Rate*

To estimate the GRB formation rate from the (z, L') data set, we again produce a cumulative number distribution $\psi(z)$ as a function of z, using a formula analogous to equation (6). In this case, the associated set should be given as

$$J'_i = \{ j \mid z_j < z_i, L_j > L_{i,\lim} \}, \tag{8}$$

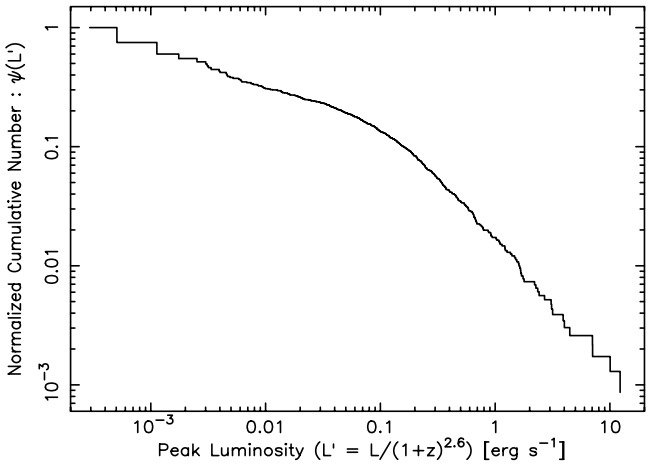

FIG. 6.—Cumulative luminosity function $\psi(L')$ of $L' = L/(1+z)^{2.60}$, which is normalized to unity at the dimmest point. This luminosity function is equivalent to the *present* luminosity function, because the effect of luminosity evolution is removed.

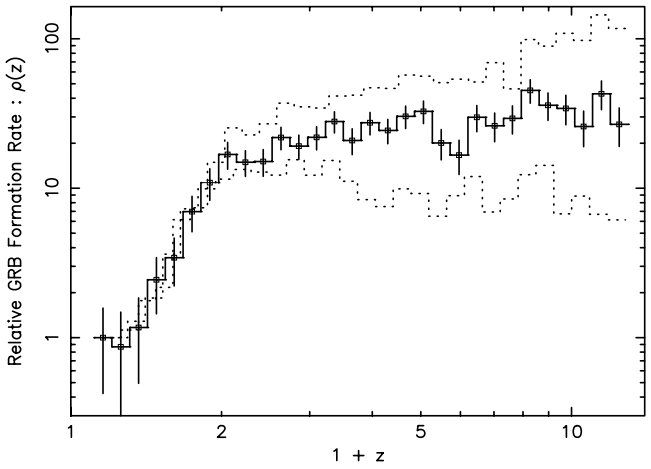

FIG. 8.—Relative GRB formation rate normalized at the first point. The solid line is the result based on the best fit of the E_p-luminosity relation. Two dotted lines indicate the upper and lower bounds caused by the uncertainty of the E_p-luminosity relation, and they are also normalized at the first point. The error bars accompanying the open squares represent the 1 σ statistical uncertainty of each point.

where $L_{i,\lim}$ is determined at the crossing point of the flux limit and $z = z_i$. We show the cumulative GRB formation rate $\psi(z)$ in Figure 7.

The differential (not the cumulative) form of the GRB formation rate is more useful for the purpose of comparison with the SFRs in other wave bands. So we convert $\psi(z)$ into the differential form with the following equation:

$$\rho(z) = \frac{d\psi(z)}{dz}(1+z)\left[\frac{dV(z)}{dz}\right]^{-1}, \tag{9}$$

where the additional factor of $(1+z)$ comes from the cosmological time dilation, and $dV(z)/dz$ is a differential comoving volume. In Figure 8 we show the relative GRB formation rate $\rho(z)$. The best result is described by

$$\rho(z) \propto \begin{cases} (1+z)^{6.0\pm1.4} & \text{for } z < 1, \\ (1+z)^{0.4\pm0.2} & \text{for } z > 1. \end{cases} \tag{10}$$

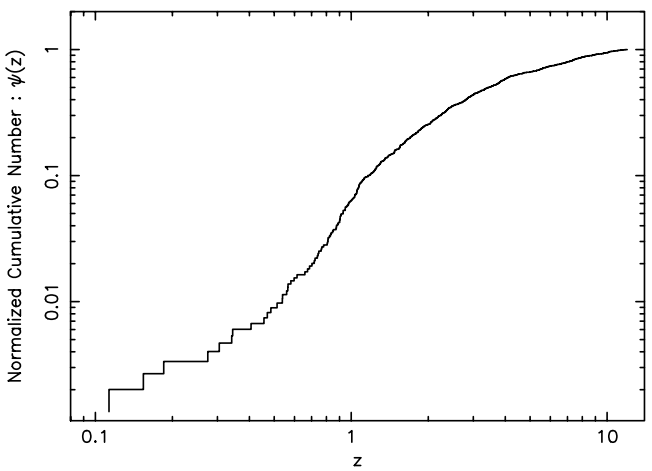

FIG. 7.—Cumulative GRB formation rate $\psi(z)$ as a function of z, which is also normalized to unity.

The upper and the lower bounds caused by the uncertainty of the E_p-luminosity relation is shown by the dotted lines.

5. DISCUSSION

We investigated the spectral properties of GRBs with known redshifts and found a high correlation between the peak energies, $E_p(1+z)$, and the peak luminosities. While the correlation to a small sample has been pointed out previously (e.g., Amati et al. 2002; Atteia 2003; Schaefer 2003a, 2003b), we have succeeded in combining the results of *BeppoSAX* and BATSE into equation (2). Although several authors mentioned the probable selection effect in the E_p-L (or E_p-F_γ) relation, we conclude that this relation is not affected by either the detector efficiency and/or their small sample selection (e.g., Amati et al. 2002; Lloyd-Ronning & Ramirez-Ruiz 2002b). The relation is an intrinsic property, but the most significant selection is the flux limit. We avoid the selection effect by using a τ statistical method and the nonparametric method of equations (5) and (6), taking into account the flux-truncation effect correctly.

Using the E_p-luminosity relation, we have estimated the redshifts of the 689 GRBs without known redshifts. However, we excluded 56 samples having larger E_p values. These samples gave extremely large distances or no solution. This might be caused by the simple linear extension of our E_p-luminosity equation toward the harder E_p and the brighter L end of the data. At present, we do not have enough information about the E_p-luminosity relation for GRBs with high E_p values, so we simply expand the E_p-luminosity relation up to $z = 12$, as was done in previous work by Fenimore & Ramirez-Ruiz (2000).

For the 689 samples, we found the existence of a luminosity evolution of $g_k(z) = (1+z)^{2.60^{+0.15}_{-0.2}}$, as shown in Figure 5. Luminosity evolutions of $(1+z)^{1.4\pm0.5}$ and $(1+z)^{1.7\pm0.5}$ were suggested independently by Lloyd-Ronning et al. (2002a) and Wei (2002). Our luminosity evolution is larger than the previous results, and this value is comparable with the luminosity evolution of QSOs. For example, Caditz & Petrosian (1990) and Maloney & Petrosian (1999) estimated the luminosity evolution of the QSO samples as $g_k(z) = (1+z)^3$ and

$(1+z)^{2.58}$, respectively. Although the validity of the functional form of the luminosity evolution should be considered, there is a possibility of the existence of a strong luminosity evolution for GRBs such as that of QSOs.

The shape of the cumulative luminosity function is independent of the redshift, except for the value of the break luminosity, which changes with z. We propose that the broken power-law shape in Figure 6 might suggest important information about the jets parameters, which is responsible for the prompt gamma-ray emissions and the distribution of their opening angles. Let us consider a simple model for a uniform jet with an opening half-angle θ_j and a constant geometrically corrected luminosity L_0, which is viewed from an angle of θ_v. Then, a crude approximation of the luminosity L is given by

$$L = \begin{cases} 2\,L_0\theta_j^{-2} & \text{for } \theta_v < \theta_j, \\ 2\,L_0(\theta_j^6/\theta_v^8) & \text{for } \theta_v > \theta_j. \end{cases} \tag{11}$$

For the case of $\theta_v > \theta_j$, L is proportional to δ^4, where $\delta = [\gamma(1-\beta\cos\theta_v)]^{-1} \propto \theta_v^{-2}$, so that the luminosity has the dependence of θ_v^{-8} (Ioka & Nakamura 2001; Yamazaki et al. 2002, 2003). The dependence of θ_j^6 is determined in order that the two functions in equation (11) are continuously connected at $\theta_v = \theta_j$. We also consider a distribution of θ_j in the form $f(\theta_j)d\theta_j \propto \theta_j^{-q}d\theta_j$ when $\theta_{\min} < \theta_j < \theta_{\max}$. Then, in the case of $q < 5/2$, we have

$$N(>L) \propto \begin{cases} L^{-1/4} & \text{for } L < 2L_0\theta_{\max}^{-2}, \\ L^{(q-3)/2} & \text{for } 2L_0\theta_{\max}^{-2} < L < 2L_0\theta_{\min}^{-2} \end{cases} \tag{12}$$

This is a broken power law with the break luminosity $2L_0\theta_{\max}^{-2}$. Then, if $\theta_{\max}^{-2}L_0 \propto g_k(z)$ with $q = 1.0$, we can roughly reproduce Figure 6. This suggests that either the maximum opening half angle of the jet decreases or the value L_0 increases as a function of the redshift.

The present work is the first study to estimate the GRB formation rate using the new E_p-luminosity relation. The result indicates that the GRB formation rate does not decrease toward $z \sim 12$. This tendency is consistent with previous works using GRB variability (Fenimore & Ramirez-Ruiz 2000; Lloyd-Ronning et al. 2002a) and the spectral time lag (Norris et al. 2000; Schaefer et al. 2001; Murakami et al. 2003). On the other hand, the SFRs measured in UV, optical, and infrared tend to decrease (or keep constant) at the higher redshift of $z \geq 2$. Currently, it is widely believed that the origin of the long-duration GRBs is the collapse of a massive star (Hjorth et al. 2003; Price et al. 2003; Uemura et al. 2003; Stanek et al. 2003). Hence our result may imply that either the formation rate of massive stars or the fraction of GRB progenitors in massive stars at high redshift should be significantly larger than the present value. However, to estimate the SFR from the observed GRB formation rate, we have to consider the jet collimation degree and also the metallicity at high redshift to compare with the SFR by Lloyd-Ronning et al. (2002a).

The existence of the luminosity evolution of GRBs, i.e., $g_k(z) = (1+z)^{2.60}$, may suggest the evolution of the GRB progenitor itself (e.g., mass, gravitational energy release) or the jet evolution. Although the jet opening angle evolution was suggested by Lloyd-Ronning et al. (2002a), our simple model shown by equation (12) may give either the maximum jet opening angle decreases or the total jet energy increases. In the former case, the GRB formation rate shown in Figure 8 may be an underestimate since the chance probability of observing a high-redshift GRB will decrease. If so, the GRB formation rate may increase more rapidly toward higher redshift. On the other hand, in the latter case, the functional form of the GRB formation rate in Figure 8 is a reasonable estimate.

Metallicity, the fraction of heavy elements, significantly contributes to the initial mass function (IMF) and stellar evolution (MacFadyen & Woosley 1999; Fryer et al. 1999). Especially, the massive star formation rate (GRB progenitor) in the total SFR highly depends on the IMF. As a simple assumption, considering the case that the metallicity decreases and the IMF flattens toward higher redshift, a careful estimation of the SFR from the GRB formation rate was done by Lloyd-Ronning et al. (2002a). To refer to their results, the derived SFR, rather than the GRB formation rate, may decrease at high redshift, as shown in Figure 8.

Both the jet angle evolution and metallicity are very important for estimating the real SFR from the observed GRB formation rate, but their dependency on the redshift is still in debate, and there are large ambiguities. Therefore, in this paper we show only the observational results of the luminosity function and the GRB formation rate.

We gratefully thank the anonymous referee for careful reading and many important suggestions to improve this paper. We thank the HEASOFT help desk, especially Bryan K. Irby, for support with the BATSE analysis tools. This research was supported by Grants-in-Aid from the Japanese Ministry of Education, Culture, Sports, Science and Technology (15740149, 14204024, 14047212, and 12640302). R. Y., A. K. I., and K. I. are supported by JSPS Research Fellowship for Young Scientists.

TABLE 2

REDSHIFTS AND LUMINOSITIES ESTIMATED BY THE E_p-LUMINOSITY RELATION

Trigger Number	E_p (keV)	Redshift	Luminosity (ergs s^{-1})
105	$141.4^{+7.8}_{-7.5}$	$1.26^{+0.11}_{-0.10}$	$(2.39^{+0.52}_{-0.43}) \times 10^{52}$
109	$385.4^{+20.7}_{-18.8}$	$1.98^{+0.20}_{-0.17}$	$(3.10^{+0.82}_{-0.60}) \times 10^{53}$
111	$97.2^{+21.7}_{-20.6}$	$11.23^{+33.87}_{-6.51}$	$(3.32^{+67.19}_{-2.87}) \times 10^{53}$
130	$182.2^{+7.4}_{-7.1}$	$5.17^{+0.68}_{-0.57}$	$(2.97^{+0.99}_{-0.71}) \times 10^{53}$
133	$73.9^{+25.4}_{-28.3}$	$4.53^{+9.47}_{-2.89}$	$(3.92^{+48.15}_{-3.58}) \times 10^{52}$
143	$620.8^{+10.8}_{-10.5}$	$1.36^{+0.04}_{-0.03}$	$(5.04^{+0.33}_{-0.31}) \times 10^{53}$
160	$207.9^{+16.5}_{-15.2}$	$4.39^{+1.10}_{-0.78}$	$(2.94^{+2.03}_{-1.10}) \times 10^{53}$
179	$198.2^{+29.4}_{-27.6}$	$8.46^{+8.12}_{-3.41}$	$(8.24^{+29.32}_{-5.74}) \times 10^{53}$
219	$20.9^{+9.2}_{-9.6}$	$0.11^{+0.05}_{-0.05}$	$(1.27^{+1.58}_{-0.94}) \times 10^{50}$
222	$280.7^{+41.1}_{-45.3}$	$9.70^{+10.46}_{-4.55}$	$(2.12^{+8.76}_{-1.62}) \times 10^{54}$
228	$42.1^{+14.9}_{-21.9}$	$1.09^{+0.65}_{-0.65}$	$(1.82^{+3.90}_{-1.62}) \times 10^{51}$
249	$261.1^{+10.5}_{-10.0}$	$1.05^{+0.06}_{-0.06}$	$(6.75^{+0.99}_{-0.83}) \times 10^{52}$
332	$84.0^{+17.3}_{-14.8}$	$3.88^{+2.90}_{-1.38}$	$(3.95^{+10.65}_{-2.56}) \times 10^{52}$
351	$59.4^{+40.5}_{-26.1}$	$1.07^{+1.47}_{-0.56}$	$(3.56^{+25.82}_{-2.96}) \times 10^{51}$
394	$323.6^{+9.0}_{-8.8}$	$7.30^{+0.80}_{-0.68}$	$(1.69^{+0.46}_{-0.34}) \times 10^{54}$
398	$122.9^{+39.7}_{-34.6}$	$5.11^{+11.11}_{-2.79}$	$(1.32^{+17.09}_{-1.12}) \times 10^{53}$
408	$75.1^{+14.0}_{-13.2}$	$2.34^{+1.03}_{-0.68}$	$(1.47^{+2.08}_{-0.84}) \times 10^{52}$
451	$134.4^{+8.3}_{-7.8}$	$0.76^{+0.06}_{-0.05}$	$(1.32^{+0.27}_{-0.22}) \times 10^{52}$
467	$311.3^{+25.6}_{-22.9}$	$7.22^{+2.69}_{-1.65}$	$(1.54^{+1.63}_{-0.69}) \times 10^{54}$
469	$227.8^{+166.6}_{-84.9}$	$3.16^{+25.84}_{-1.81}$	$(2.11^{+326.44}_{-1.84}) \times 10^{53}$
493	$144.2^{+25.4}_{-33.0}$	$11.94^{+22.92}_{-7.34}$	$(8.16^{+78.59}_{-7.25}) \times 10^{53}$
501	$72.5^{+10.2}_{-6.7}$	$2.40^{+0.77}_{-0.40}$	$(1.43^{+1.37}_{-0.51}) \times 10^{52}$
503	$494.7^{+65.1}_{-52.3}$	$6.10^{+3.65}_{-1.74}$	$(2.90^{+5.60}_{-1.58}) \times 10^{54}$
543	$253.0^{+8.7}_{-8.3}$	$2.54^{+0.18}_{-0.16}$	$(1.88^{+0.35}_{-0.28}) \times 10^{53}$
548	$158.3^{+13.4}_{-12.5}$	$10.10^{+5.08}_{-2.86}$	$(7.24^{+10.87}_{-3.86}) \times 10^{53}$
577	$117.0^{+36.2}_{-27.2}$	$5.58^{+12.48}_{-2.76}$	$(1.39^{+18.63}_{-1.11}) \times 10^{53}$
647	$200.6^{+6.0}_{-5.9}$	$3.11^{+0.22}_{-0.20}$	$(1.59^{+0.28}_{-0.23}) \times 10^{53}$
658	$88.1^{+25.4}_{-31.2}$	$3.91^{+4.96}_{-2.29}$	$(4.39^{+25.05}_{-3.87}) \times 10^{52}$
659	$62.2^{+1.6}_{-15.6}$	$2.82^{+0.16}_{-1.18}$	$(1.33^{+0.19}_{-0.97}) \times 10^{52}$
660	$282.8^{+27.2}_{-24.1}$	$9.23^{+5.11}_{-2.66}$	$(1.96^{+3.34}_{-1.06}) \times 10^{54}$
676	$321.1^{+10.1}_{-9.9}$	$9.69^{+1.47}_{-1.19}$	$(2.76^{+1.04}_{-0.71}) \times 10^{54}$
680	$82.1^{+30.0}_{-26.0}$	$4.33^{+9.59}_{-2.43}$	$(4.49^{+61.16}_{-3.87}) \times 10^{52}$
692	$107.1^{+25.0}_{-21.9}$	$9.65^{+25.63}_{-5.23}$	$(3.05^{+50.85}_{-2.55}) \times 10^{53}$
704	$132.7^{+30.5}_{-13.6}$	$3.69^{+3.10}_{-0.82}$	$(9.09^{+28.80}_{-4.10}) \times 10^{52}$
764	$100.6^{+11.4}_{-29.6}$	$5.93^{+2.85}_{-3.46}$	$(1.14^{+1.68}_{-1.00}) \times 10^{53}$
773	$70.9^{+21.4}_{-9.9}$	$2.25^{+1.79}_{-0.53}$	$(1.24^{+3.82}_{-0.60}) \times 10^{52}$
795	$109.3^{+32.6}_{-31.7}$	$6.95^{+20.01}_{-4.20}$	$(1.77^{+35.18}_{-1.57}) \times 10^{53}$
825	$71.1^{+36.9}_{-27.8}$	$3.21^{+9.82}_{-1.91}$	$(2.10^{+51.85}_{-1.87}) \times 10^{52}$
829	$127.7^{+0.8}_{-1.2}$	$1.85^{+0.02}_{-0.03}$	$(3.11^{+0.08}_{-0.13}) \times 10^{52}$
841	$102.2^{+12.8}_{-11.1}$	$1.30^{+0.26}_{-0.20}$	$(1.30^{+0.75}_{-0.44}) \times 10^{52}$
869	$235.2^{+28.7}_{-25.8}$	$8.03^{+5.50}_{-2.66}$	$(1.06^{+2.39}_{-0.64}) \times 10^{54}$
907	$211.9^{+7.4}_{-7.1}$	$4.98^{+0.55}_{-0.47}$	$(3.77^{+1.05}_{-0.78}) \times 10^{53}$
914	$88.8^{+17.3}_{-16.3}$	$1.70^{+0.64}_{-0.46}$	$(1.35^{+1.60}_{-0.73}) \times 10^{52}$
973	$289.4^{+11.9}_{-11.4}$	$4.72^{+0.60}_{-0.50}$	$(6.44^{+2.08}_{-1.48}) \times 10^{53}$
999	$262.8^{+17.8}_{-16.1}$	$1.72^{+0.21}_{-0.17}$	$(1.20^{+0.38}_{-0.27}) \times 10^{53}$
1025	$153.2^{+7.5}_{-7.1}$	$1.18^{+0.09}_{-0.08}$	$(2.62^{+0.50}_{-0.40}) \times 10^{52}$
1036	$99.7^{+33.2}_{-28.7}$	$3.14^{+3.97}_{-1.51}$	$(4.00^{+23.27}_{-3.18}) \times 10^{52}$
1039	$93.9^{+3.8}_{-3.5}$	$5.51^{+0.76}_{-0.60}$	$(8.78^{+3.08}_{-2.09}) \times 10^{52}$
1042	$47.9^{+7.4}_{-6.4}$	$1.30^{+0.33}_{-0.24}$	$(2.85^{+2.11}_{-1.14}) \times 10^{51}$
1085	$227.2^{+1.9}_{-1.8}$	$0.93^{+0.01}_{-0.01}$	$(4.50^{+0.12}_{-0.12}) \times 10^{52}$
1114	$106.2^{+8.1}_{-7.6}$	$4.29^{+1.00}_{-0.75}$	$(7.39^{+4.72}_{-2.69}) \times 10^{52}$
1122	$170.7^{+4.7}_{-4.5}$	$1.54^{+0.07}_{-0.07}$	$(4.42^{+0.50}_{-0.44}) \times 10^{52}$
1141	$417.6^{+9.9}_{-9.6}$	$6.25^{+0.52}_{-0.46}$	$(2.15^{+0.44}_{-0.35}) \times 10^{54}$
1145	$77.7^{+28.6}_{-48.2}$	$2.56^{+3.07}_{-1.96}$	$(1.80^{+9.87}_{-1.75}) \times 10^{52}$
1148	$191.6^{+33.7}_{-39.1}$	$9.77^{+14.63}_{-5.31}$	$(9.98^{+66.86}_{-8.36}) \times 10^{53}$
1150	$66.5^{+3.6}_{-3.0}$	$1.54^{+0.14}_{-0.11}$	$(6.71^{+1.57}_{-1.10}) \times 10^{51}$
1156	$87.6^{+33.0}_{-29.5}$	$6.93^{+38.83}_{-4.55}$	$(1.13^{+73.50}_{-1.04}) \times 10^{53}$
1157	$236.8^{+9.5}_{-9.1}$	$1.82^{+0.13}_{-0.12}$	$(1.05^{+0.19}_{-0.16}) \times 10^{53}$
1159	$254.4^{+23.1}_{-20.1}$	$9.96^{+5.45}_{-2.80}$	$(1.82^{+3.04}_{-0.97}) \times 10^{54}$
1190	$121.9^{+12.5}_{-11.7}$	$2.67^{+0.64}_{-0.48}$	$(4.70^{+3.18}_{-1.80}) \times 10^{52}$
1197	$92.3^{+32.6}_{-39.8}$	$3.70^{+6.25}_{-2.42}$	$(4.43^{+39.50}_{-4.09}) \times 10^{52}$
1200	$90.1^{+18.3}_{-11.6}$	$3.98^{+3.01}_{-1.11}$	$(4.72^{+12.91}_{-2.56}) \times 10^{52}$
1218	$116.1^{+5.0}_{-5.0}$	$11.11^{+2.64}_{-1.98}$	$(4.64^{+2.85}_{-1.67}) \times 10^{53}$
1235	$122.1^{+11.5}_{-9.9}$	$2.25^{+0.44}_{-0.32}$	$(3.70^{+2.02}_{-1.17}) \times 10^{52}$

TABLE 2—*Continued*

Trigger Number	E_p (keV)	Redshift	Luminosity (ergs s^{-1})
1244	$30.7^{+39.0}_{-23.9}$	$0.85^{+2.47}_{-0.69}$	$(7.55^{+204.68}_{-7.40}) \times 10^{50}$
1288	$354.7^{+24.3}_{-22.8}$	$9.29^{+3.34}_{-2.13}$	$(3.13^{+3.14}_{-1.41}) \times 10^{54}$
1303	$195.5^{+31.6}_{-52.9}$	$11.00^{+16.12}_{-7.21}$	$(1.29^{+8.27}_{-1.18}) \times 10^{54}$
1384	$103.5^{+15.1}_{-20.7}$	$8.14^{+7.34}_{-4.13}$	$(2.10^{+6.87}_{-1.70}) \times 10^{53}$
1396	$105.9^{+23.5}_{-24.3}$	$4.05^{+3.53}_{-1.78}$	$(6.70^{+22.19}_{-5.04}) \times 10^{52}$
1406	$106.9^{+10.8}_{-13.4}$	$1.91^{+0.37}_{-0.39}$	$(2.28^{+1.23}_{-0.97}) \times 10^{52}$
1416	$104.3^{+32.4}_{-28.7}$	$2.96^{+3.15}_{-1.34}$	$(4.00^{+18.13}_{-3.08}) \times 10^{52}$
1419	$145.6^{+32.5}_{-27.3}$	$2.31^{+1.27}_{-0.71}$	$(5.46^{+10.19}_{-3.24}) \times 10^{52}$
1425	$185.9^{+9.3}_{-8.9}$	$2.19^{+0.21}_{-0.19}$	$(8.23^{+2.11}_{-1.63}) \times 10^{52}$
1432	$62.3^{+22.5}_{-16.0}$	$2.91^{+3.88}_{-1.25}$	$(1.39^{+8.85}_{-1.04}) \times 10^{52}$
1440	$271.2^{+6.7}_{-6.5}$	$2.52^{+0.13}_{-0.12}$	$(2.14^{+0.28}_{-0.24}) \times 10^{53}$
1443	$163.3^{+29.0}_{-25.1}$	$3.47^{+1.95}_{-1.06}$	$(1.25^{+2.32}_{-0.73}) \times 10^{53}$
1467	$140.8^{+47.6}_{-30.3}$	$2.33^{+2.25}_{-0.81}$	$(5.15^{+20.77}_{-3.34}) \times 10^{52}$
1472	$142.7^{+21.7}_{-19.5}$	$9.64^{+10.99}_{-4.04}$	$(5.41^{+24.24}_{-3.86}) \times 10^{53}$
1533	$149.9^{+25.3}_{-23.2}$	$3.28^{+1.65}_{-0.98}$	$(9.68^{+15.70}_{-5.57}) \times 10^{52}$
1540	$112.7^{+16.8}_{-20.5}$	$7.54^{+6.53}_{-3.51}$	$(2.17^{+6.76}_{-1.67}) \times 10^{53}$
1541	$39.8^{+48.8}_{-15.5}$	$0.18^{+0.26}_{-0.07}$	$(5.17^{+33.14}_{-3.47}) \times 10^{50}$
1574	$98.5^{+20.7}_{-7.2}$	$6.92^{+9.62}_{-1.54}$	$(1.43^{+8.83}_{-0.63}) \times 10^{53}$
1578	$179.8^{+9.4}_{-8.9}$	$3.75^{+0.54}_{-0.43}$	$(1.71^{+0.64}_{-0.43}) \times 10^{53}$
1579	$314.0^{+169.9}_{-88.5}$	$2.11^{+3.90}_{-0.89}$	$(2.24^{+24.82}_{-1.65}) \times 10^{53}$
1614	$144.8^{+31.7}_{-35.7}$	$7.56^{+12.58}_{-4.26}$	$(3.60^{+29.05}_{-3.09}) \times 10^{53}$
1625	$580.6^{+8.4}_{-8.2}$	$2.20^{+0.06}_{-0.06}$	$(8.10^{+0.56}_{-0.51}) \times 10^{53}$
1626	$157.7^{+36.7}_{-29.8}$	$7.45^{+13.67}_{-3.54}$	$(4.16^{+39.19}_{-3.24}) \times 10^{53}$
1628	$133.1^{+44.2}_{-50.0}$	$5.33^{+13.01}_{-3.49}$	$(1.67^{+25.92}_{-1.54}) \times 10^{53}$
1651	$56.3^{+17.7}_{-24.8}$	$0.54^{+0.21}_{-0.26}$	$(1.75^{+2.17}_{-1.37}) \times 10^{51}$
1652	$184.8^{+7.6}_{-7.3}$	$2.95^{+0.28}_{-0.24}$	$(1.25^{+0.30}_{-0.23}) \times 10^{53}$
1660	$90.4^{+33.4}_{-18.9}$	$2.00^{+1.91}_{-0.64}$	$(1.72^{+6.92}_{-1.06}) \times 10^{52}$
1663	$448.7^{+8.9}_{-8.3}$	$2.78^{+0.12}_{-0.11}$	$(6.74^{+0.72}_{-0.61}) \times 10^{53}$
1683	$353.2^{+17.1}_{-16.2}$	$11.69^{+3.26}_{-2.26}$	$(4.71^{+3.47}_{-1.81}) \times 10^{54}$
1709	$204.6^{+5.6}_{-5.5}$	$2.00^{+0.10}_{-0.10}$	$(8.83^{+1.13}_{-0.99}) \times 10^{52}$
1712	$212.3^{+23.1}_{-21.5}$	$10.31^{+7.46}_{-3.57}$	$(1.35^{+3.23}_{-0.84}) \times 10^{54}$
1717	$166.4^{+15.7}_{-14.0}$	$4.48^{+1.39}_{-0.91}$	$(1.95^{+1.72}_{-0.81}) \times 10^{53}$
1734	$90.0^{+22.2}_{-20.3}$	$3.81^{+3.66}_{-1.63}$	$(4.40^{+16.84}_{-3.24}) \times 10^{52}$
1807	$149.6^{+14.9}_{-21.5}$	$4.11^{+1.28}_{-1.27}$	$(1.37^{+1.22}_{-0.81}) \times 10^{53}$
1815	$201.1^{+24.8}_{-20.8}$	$3.21^{+1.08}_{-0.68}$	$(1.68^{+1.67}_{-0.73}) \times 10^{53}$
1883	$211.6^{+10.6}_{-10.2}$	$3.25^{+0.40}_{-0.34}$	$(1.90^{+0.61}_{-0.44}) \times 10^{53}$
1885	$103.8^{+30.8}_{-41.8}$	$8.17^{+30.64}_{-6.05}$	$(2.13^{+65.28}_{-2.04}) \times 10^{53}$
1886	$488.8^{+6.5}_{-6.4}$	$2.10^{+0.05}_{-0.05}$	$(5.38^{+0.33}_{-0.31}) \times 10^{53}$
1922	$170.0^{+27.6}_{-25.4}$	$10.21^{+13.88}_{-4.63}$	$(8.52^{+49.17}_{-6.40}) \times 10^{53}$
1924	$80.0^{+22.8}_{-41.2}$	$2.29^{+1.71}_{-1.52}$	$(1.62^{+4.58}_{-1.51}) \times 10^{52}$
1956	$143.8^{+18.5}_{-16.5}$	$4.47^{+2.02}_{-1.19}$	$(1.45^{+2.02}_{-0.76}) \times 10^{53}$
1967	$119.5^{+7.8}_{-7.0}$	$5.28^{+1.20}_{-0.85}$	$(1.32^{+0.86}_{-0.45}) \times 10^{53}$
1974	$53.8^{+3.3}_{-2.5}$	$0.67^{+0.05}_{-0.04}$	$(1.90^{+0.38}_{-0.26}) \times 10^{51}$
1989	$97.4^{+24.0}_{-11.6}$	$1.98^{+1.10}_{-0.38}$	$(1.97^{+3.76}_{-0.81}) \times 10^{52}$
1993	$57.1^{+2.8}_{-12.4}$	$1.62^{+0.14}_{-0.50}$	$(5.25^{+1.14}_{-3.15}) \times 10^{51}$
1997	$31.0^{+14.5}_{-11.4}$	$0.28^{+0.14}_{-0.11}$	$(3.65^{+6.11}_{-2.42}) \times 10^{50}$
2018	$53.4^{+3.6}_{-2.7}$	$1.79^{+0.22}_{-0.15}$	$(5.22^{+1.67}_{-1.01}) \times 10^{51}$
2037	$103.9^{+35.1}_{-22.2}$	$0.57^{+0.24}_{-0.14}$	$(6.20^{+8.67}_{-3.00}) \times 10^{51}$
2047	$70.0^{+18.6}_{-24.5}$	$1.63^{+0.87}_{-0.76}$	$(7.94^{+14.55}_{-6.25}) \times 10^{51}$
2053	$186.6^{+17.4}_{-21.6}$	$7.93^{+3.74}_{-2.72}$	$(6.51^{+9.17}_{-4.05}) \times 10^{53}$
2061	$223.8^{+58.8}_{-56.1}$	$4.53^{+5.75}_{-2.21}$	$(3.60^{+20.28}_{-2.87}) \times 10^{53}$
2067	$271.2^{+2.3}_{-2.3}$	$1.77^{+0.03}_{-0.03}$	$(1.32^{+0.05}_{-0.05}) \times 10^{53}$
2074	$139.8^{+57.3}_{-41.1}$	$5.30^{+21.63}_{-3.00}$	$(1.82^{+69.21}_{-1.57}) \times 10^{53}$
2080	$345.8^{+30.0}_{-27.6}$	$11.55^{+6.69}_{-3.49}$	$(4.42^{+7.84}_{-2.47}) \times 10^{54}$
2083	$332.5^{+4.9}_{-4.8}$	$1.06^{+0.02}_{-0.02}$	$(1.10^{+0.06}_{-0.05}) \times 10^{53}$
2090	$230.1^{+8.6}_{-8.3}$	$2.46^{+0.19}_{-0.17}$	$(1.48^{+0.29}_{-0.24}) \times 10^{53}$
2102	$134.2^{+27.4}_{-20.5}$	$4.84^{+4.40}_{-1.68}$	$(1.44^{+4.98}_{-0.92}) \times 10^{53}$
2106	$174.8^{+28.2}_{-19.6}$	$8.01^{+8.35}_{-2.69}$	$(5.83^{+23.34}_{-3.56}) \times 10^{53}$
2111	$105.5^{+5.1}_{-16.2}$	$7.90^{+1.68}_{-3.32}$	$(2.07^{+1.14}_{-1.49}) \times 10^{53}$
2119	$136.9^{+7.6}_{-9.0}$	$8.36^{+2.18}_{-1.87}$	$(3.85^{+2.67}_{-1.70}) \times 10^{53}$
2122	$101.9^{+39.0}_{-26.8}$	$1.30^{+0.94}_{-0.45}$	$(1.29^{+3.62}_{-0.84}) \times 10^{52}$
2123	$104.3^{+15.7}_{-14.8}$	$3.48^{+1.59}_{-1.00}$	$(5.12^{+7.32}_{-2.84}) \times 10^{52}$
2138	$238.4^{+19.9}_{-12.0}$	$2.46^{+0.45}_{-0.24}$	$(1.60^{+0.80}_{-0.35}) \times 10^{53}$
2148	$90.0^{+54.4}_{-56.9}$	$2.27^{+5.65}_{-1.72}$	$(2.03^{+36.89}_{-1.97}) \times 10^{52}$
2151	$146.8^{+3.6}_{-3.5}$	$0.30^{+0.01}_{-0.01}$	$(8.60^{+0.53}_{-0.51}) \times 10^{51}$

TABLE 2—*Continued*

Trigger Number	E_p (keV)	Redshift	Luminosity (ergs s^{-1})
2156	$381.2^{+9.8}_{-9.4}$	$2.40^{+0.12}_{-0.11}$	$(3.94^{+0.51}_{-0.44}) \times 10^{53}$
2188	$97.7^{+14.5}_{-22.2}$	$10.20^{+11.82}_{-5.97}$	$(2.81^{+12.83}_{-2.44}) \times 10^{53}$
2197	$50.5^{+35.3}_{-30.5}$	$1.72^{+3.96}_{-1.23}$	$(4.43^{+72.63}_{-4.22}) \times 10^{51}$
2211	$103.0^{+2.3}_{-14.4}$	$2.78^{+0.14}_{-0.72}$	$(3.55^{+0.44}_{-1.83}) \times 10^{52}$
2213	$300.5^{+27.3}_{-25.5}$	$9.97^{+5.45}_{-2.96}$	$(2.55^{+4.24}_{-1.41}) \times 10^{54}$
2228	$192.7^{+14.7}_{-13.3}$	$2.18^{+0.34}_{-0.27}$	$(8.83^{+3.69}_{-2.41}) \times 10^{52}$
2232	$228.3^{+35.4}_{-32.6}$	$3.87^{+1.99}_{-1.16}$	$(2.90^{+4.77}_{-1.67}) \times 10^{53}$
2253	$117.2^{+13.1}_{-22.2}$	$7.86^{+4.69}_{-3.81}$	$(2.53^{+4.78}_{-1.99}) \times 10^{53}$
2254	$147.6^{+23.4}_{-34.5}$	$3.41^{+1.64}_{-1.44}$	$(9.96^{+15.18}_{-7.31}) \times 10^{52}$
2267	$83.6^{+42.5}_{-43.9}$	$3.03^{+8.03}_{-2.14}$	$(2.66^{+51.53}_{-2.53}) \times 10^{52}$
2276	$32.3^{+15.4}_{-14.7}$	$0.88^{+0.66}_{-0.45}$	$(8.60^{+25.57}_{-7.13}) \times 10^{50}$
2277	$157.4^{+10.0}_{-30.4}$	$9.83^{+3.37}_{-5.19}$	$(6.81^{+6.45}_{-5.61}) \times 10^{53}$
2287	$139.9^{+35.8}_{-31.9}$	$3.81^{+3.86}_{-1.63}$	$(1.06^{+4.38}_{-0.79}) \times 10^{53}$
2309	$207.4^{+28.1}_{-37.0}$	$8.70^{+7.47}_{-4.19}$	$(9.49^{+28.89}_{-7.43}) \times 10^{53}$
2315	$165.4^{+9.9}_{-9.4}$	$10.48^{+3.48}_{-2.30}$	$(8.46^{+7.67}_{-3.64}) \times 10^{53}$
2316	$138.6^{+1.5}_{-1.3}$	$2.05^{+0.04}_{-0.03}$	$(4.19^{+0.21}_{-0.17}) \times 10^{52}$
2321	$208.0^{+7.8}_{-7.5}$	$2.64^{+0.21}_{-0.19}$	$(1.35^{+0.28}_{-0.22}) \times 10^{53}$
2328	$125.4^{+21.6}_{-17.9}$	$5.60^{+4.54}_{-1.96}$	$(1.61^{+4.68}_{-1.02}) \times 10^{53}$
2329	$896.8^{+12.2}_{-11.9}$	$2.64^{+0.07}_{-0.07}$	$(2.49^{+0.17}_{-0.16}) \times 10^{54}$
2340	$109.7^{+5.9}_{-6.3}$	$3.88^{+0.58}_{-0.52}$	$(6.73^{+2.64}_{-1.96}) \times 10^{52}$
2345	$129.4^{+25.4}_{-20.5}$	$4.17^{+3.12}_{-1.40}$	$(1.05^{+2.81}_{-0.65}) \times 10^{53}$
2346	$116.7^{+24.7}_{-22.1}$	$2.46^{+1.32}_{-0.78}$	$(3.83^{+6.89}_{-2.32}) \times 10^{52}$
2362	$65.0^{+5.0}_{-5.7}$	$1.03^{+0.11}_{-0.12}$	$(4.09^{+1.20}_{-1.07}) \times 10^{51}$
2367	$134.2^{+10.2}_{-16.6}$	$3.83^{+0.84}_{-1.02}$	$(9.88^{+5.88}_{-5.15}) \times 10^{52}$
2380	$89.5^{+40.3}_{-42.9}$	$4.02^{+12.71}_{-2.84}$	$(4.73^{+119.38}_{-4.49}) \times 10^{52}$
2387	$181.7^{+8.4}_{-8.0}$	$3.76^{+0.47}_{-0.39}$	$(1.76^{+0.56}_{-0.40}) \times 10^{53}$
2393	$53.2^{+2.0}_{-2.1}$	$0.75^{+0.04}_{-0.04}$	$(2.02^{+0.25}_{-0.23}) \times 10^{51}$
2394	$161.9^{+31.2}_{-33.0}$	$8.19^{+11.83}_{-4.22}$	$(5.20^{+33.52}_{-4.23}) \times 10^{53}$
2423	$67.6^{+26.2}_{-33.5}$	$2.74^{+3.83}_{-1.84}$	$(1.50^{+10.34}_{-1.40}) \times 10^{52}$
2429	$127.3^{+52.4}_{-61.1}$	$5.57^{+25.58}_{-4.17}$	$(1.64^{+76.72}_{-1.58}) \times 10^{53}$
2430	$53.5^{+27.1}_{-28.9}$	$1.29^{+1.34}_{-0.81}$	$(3.51^{+16.56}_{-3.20}) \times 10^{51}$
2431	$96.2^{+15.3}_{-14.0}$	$0.47^{+0.09}_{-0.08}$	$(4.68^{+2.41}_{-1.61}) \times 10^{51}$
2432	$61.1^{+33.6}_{-21.8}$	$1.48^{+1.93}_{-0.69}$	$(5.38^{+35.50}_{-4.22}) \times 10^{51}$
2435	$105.2^{+19.8}_{-26.3}$	$2.50^{+1.18}_{-1.00}$	$(3.19^{+4.84}_{-2.27}) \times 10^{52}$
2436	$320.2^{+49.0}_{-73.8}$	$6.88^{+5.68}_{-3.62}$	$(1.49^{+4.39}_{-1.23}) \times 10^{54}$
2438	$64.1^{+3.6}_{-3.8}$	$1.26^{+0.11}_{-0.11}$	$(4.94^{+1.10}_{-0.97}) \times 10^{51}$
2443	$180.9^{+28.2}_{-22.1}$	$3.08^{+1.33}_{-0.74}$	$(1.28^{+1.72}_{-0.62}) \times 10^{53}$
2446	$276.0^{+11.8}_{-11.4}$	$10.12^{+2.23}_{-1.65}$	$(2.21^{+1.25}_{-0.74}) \times 10^{54}$
2451	$153.9^{+43.2}_{-36.1}$	$5.49^{+9.83}_{-2.72}$	$(2.34^{+21.93}_{-1.88}) \times 10^{53}$
2453	$81.9^{+12.7}_{-15.0}$	$4.68^{+2.82}_{-1.84}$	$(5.09^{+10.11}_{-3.54}) \times 10^{52}$
2458	$28.7^{+40.4}_{-11.2}$	$0.56^{+1.36}_{-0.24}$	$(4.74^{+91.21}_{-3.49}) \times 10^{50}$
2460	$73.0^{+27.9}_{-48.3}$	$3.35^{+5.77}_{-2.73}$	$(2.36^{+22.08}_{-2.32}) \times 10^{52}$
2476	$65.3^{+1.3}_{-1.4}$	$1.43^{+0.04}_{-0.05}$	$(5.89^{+0.46}_{-0.46}) \times 10^{51}$
2477	$118.0^{+4.1}_{-7.0}$	$11.06^{+2.02}_{-2.59}$	$(4.75^{+2.18}_{-2.16}) \times 10^{53}$
2482	$118.3^{+8.4}_{-7.1}$	$7.11^{+2.21}_{-1.36}$	$(2.16^{+1.86}_{-0.84}) \times 10^{53}$
2500	$118.5^{+18.8}_{-20.2}$	$7.29^{+6.71}_{-3.20}$	$(2.26^{+7.69}_{-1.68}) \times 10^{53}$
2510	$68.5^{+46.2}_{-31.0}$	$1.48^{+2.67}_{-0.83}$	$(6.76^{+75.12}_{-5.86}) \times 10^{51}$
2511	$59.6^{+48.0}_{-39.0}$	$1.29^{+2.73}_{-0.95}$	$(4.38^{+64.15}_{-4.20}) \times 10^{51}$
2519	$148.4^{+27.5}_{-25.9}$	$10.24^{+17.93}_{-5.15}$	$(6.53^{+55.23}_{-5.22}) \times 10^{53}$
2530	$205.8^{+52.6}_{-53.8}$	$5.88^{+9.60}_{-3.19}$	$(4.70^{+37.82}_{-3.96}) \times 10^{53}$
2533	$380.4^{+5.7}_{-5.6}$	$4.36^{+0.18}_{-0.17}$	$(9.76^{+1.00}_{-0.88}) \times 10^{53}$
2537	$103.6^{+6.1}_{-5.3}$	$0.56^{+0.04}_{-0.03}$	$(6.11^{+1.08}_{-0.86}) \times 10^{51}$
2570	$212.6^{+20.8}_{-17.2}$	$3.47^{+0.94}_{-0.61}$	$(2.12^{+1.62}_{-0.78}) \times 10^{53}$
2586	$297.9^{+12.7}_{-12.1}$	$6.63^{+1.09}_{-0.86}$	$(1.21^{+0.51}_{-0.33}) \times 10^{54}$
2593	$72.3^{+4.2}_{-4.0}$	$2.21^{+0.26}_{-0.22}$	$(1.26^{+0.39}_{-0.28}) \times 10^{52}$
2600	$102.9^{+4.6}_{-11.7}$	$4.69^{+0.65}_{-1.26}$	$(8.04^{+2.86}_{-4.21}) \times 10^{52}$
2603	$82.2^{+1.3}_{-1.4}$	$1.48^{+0.04}_{-0.04}$	$(9.72^{+0.59}_{-0.64}) \times 10^{51}$
2611	$550.4^{+15.4}_{-15.2}$	$2.90^{+0.18}_{-0.17}$	$(1.08^{+0.17}_{-0.15}) \times 10^{54}$
2620	$73.7^{+4.6}_{-4.7}$	$2.72^{+0.39}_{-0.34}$	$(1.77^{+0.66}_{-0.49}) \times 10^{52}$
2628	$170.5^{+9.1}_{-9.2}$	$1.90^{+0.19}_{-0.17}$	$(5.72^{+1.48}_{-1.19}) \times 10^{52}$
2634	$51.0^{+6.8}_{-13.9}$	$0.78^{+0.14}_{-0.25}$	$(1.93^{+0.96}_{-1.18}) \times 10^{51}$
2640	$30.1^{+36.8}_{-20.1}$	$0.72^{+1.71}_{-0.51}$	$(6.28^{+116.82}_{-5.94}) \times 10^{50}$
2660	$88.2^{+12.6}_{-14.2}$	$5.63^{+3.51}_{-2.16}$	$(8.03^{+16.48}_{-5.45}) \times 10^{52}$
2662	$123.4^{+40.3}_{-28.7}$	$4.62^{+8.91}_{-2.15}$	$(1.13^{+12.17}_{-0.88}) \times 10^{53}$
2665	$98.6^{+5.9}_{-6.3}$	$1.19^{+0.11}_{-0.11}$	$(1.10^{+0.26}_{-0.23}) \times 10^{52}$

TABLE 2—*Continued*

Trigger Number	E_p (keV)	Redshift	Luminosity (ergs s^{-1})
2696	$116.8^{+14.3}_{-13.6}$	$7.67^{+5.06}_{-2.61}$	$(2.41^{+5.19}_{-1.49}) \times 10^{53}$
2697	$93.5^{+24.0}_{-25.9}$	$4.98^{+6.74}_{-2.67}$	$(7.34^{+45.08}_{-6.16}) \times 10^{52}$
2700	$197.6^{+67.4}_{-47.4}$	$2.62^{+2.85}_{-1.03}$	$(1.20^{+5.70}_{-0.84}) \times 10^{53}$
2703	$236.2^{+56.2}_{-63.1}$	$6.94^{+12.16}_{-4.00}$	$(8.25^{+72.85}_{-7.16}) \times 10^{53}$
2706	$157.4^{+23.5}_{-20.3}$	$10.43^{+12.52}_{-4.32}$	$(7.59^{+36.45}_{-5.36}) \times 10^{53}$
2709	$189.6^{+14.4}_{-13.0}$	$10.20^{+4.49}_{-2.58}$	$(1.06^{+1.34}_{-0.51}) \times 10^{54}$
2711	$101.7^{+38.0}_{-23.6}$	$5.06^{+14.89}_{-2.42}$	$(8.91^{+191.99}_{-7.02}) \times 10^{52}$
2728	$159.5^{+46.0}_{-44.8}$	$7.75^{+24.43}_{-4.74}$	$(4.57^{+104.51}_{-4.07}) \times 10^{53}$
2736	$185.4^{+38.0}_{-34.8}$	$3.53^{+2.43}_{-1.27}$	$(1.66^{+4.03}_{-1.09}) \times 10^{53}$
2749	$48.9^{+29.9}_{-8.1}$	$1.35^{+1.89}_{-0.31}$	$(3.08^{+23.10}_{-1.47}) \times 10^{51}$
2760	$65.7^{+3.9}_{-10.9}$	$2.85^{+0.39}_{-0.85}$	$(1.50^{+0.54}_{-0.87}) \times 10^{52}$
2774	$63.5^{+20.9}_{-22.4}$	$1.93^{+1.53}_{-0.94}$	$(8.13^{+25.12}_{-6.56}) \times 10^{51}$
2790	$217.1^{+16.0}_{-15.6}$	$6.77^{+2.11}_{-1.47}$	$(6.68^{+5.77}_{-2.90}) \times 10^{53}$
2797	$273.7^{+9.8}_{-9.3}$	$3.20^{+0.27}_{-0.24}$	$(3.10^{+0.67}_{-0.53}) \times 10^{53}$
2798	$536.3^{+5.6}_{-5.5}$	$2.08^{+0.04}_{-0.04}$	$(6.40^{+0.30}_{-0.29}) \times 10^{53}$
2799	$164.5^{+17.6}_{-16.6}$	$2.81^{+0.73}_{-0.54}$	$(9.23^{+6.85}_{-3.75}) \times 10^{52}$
2812	$235.7^{+7.4}_{-7.1}$	$1.93^{+0.11}_{-0.10}$	$(1.12^{+0.16}_{-0.14}) \times 10^{53}$
2815	$91.4^{+5.4}_{-5.8}$	$6.27^{+1.43}_{-1.18}$	$(1.04^{+0.63}_{-0.40}) \times 10^{53}$
2831	$766.1^{+15.9}_{-15.5}$	$1.31^{+0.04}_{-0.04}$	$(7.34^{+0.58}_{-0.54}) \times 10^{53}$
2852	$437.3^{+29.8}_{-27.3}$	$7.57^{+2.33}_{-1.54}$	$(3.30^{+2.79}_{-1.35}) \times 10^{54}$
2855	$318.2^{+6.7}_{-6.5}$	$2.16^{+0.09}_{-0.08}$	$(2.37^{+0.24}_{-0.21}) \times 10^{53}$
2877	$48.6^{+1.8}_{-1.8}$	$0.41^{+0.02}_{-0.02}$	$(1.10^{+0.11}_{-0.11}) \times 10^{51}$
2880	$137.1^{+23.5}_{-21.2}$	$3.39^{+1.77}_{-1.03}$	$(8.49^{+14.47}_{-4.93}) \times 10^{52}$
2889	$248.9^{+48.5}_{-39.0}$	$4.20^{+3.12}_{-1.40}$	$(3.93^{+10.44}_{-2.44}) \times 10^{53}$
2891	$747.5^{+19.7}_{-18.9}$	$8.81^{+1.03}_{-0.86}$	$(1.26^{+0.36}_{-0.26}) \times 10^{55}$
2894	$217.3^{+9.5}_{-8.9}$	$1.59^{+0.12}_{-0.10}$	$(7.44^{+1.40}_{-1.14}) \times 10^{52}$
2897	$45.4^{+0.9}_{-1.2}$	$0.77^{+0.02}_{-0.03}$	$(1.51^{+0.09}_{-0.12}) \times 10^{51}$
2913	$121.6^{+17.0}_{-15.7}$	$2.09^{+0.61}_{-0.45}$	$(3.31^{+2.86}_{-1.47}) \times 10^{52}$
2919	$315.6^{+23.4}_{-21.4}$	$4.22^{+0.95}_{-0.69}$	$(6.36^{+3.89}_{-2.20}) \times 10^{53}$
2924	$101.4^{+8.5}_{-8.9}$	$10.43^{+5.33}_{-3.25}$	$(3.15^{+4.81}_{-1.81}) \times 10^{53}$
2925	$73.5^{+39.4}_{-30.6}$	$3.74^{+16.43}_{-2.40}$	$(2.85^{+131.22}_{-2.62}) \times 10^{52}$
2929	$460.5^{+15.6}_{-14.8}$	$3.95^{+0.37}_{-0.31}$	$(1.22^{+0.29}_{-0.22}) \times 10^{54}$
2945	$42.8^{+14.8}_{-7.9}$	$1.39^{+0.92}_{-0.36}$	$(2.44^{+6.09}_{-1.26}) \times 10^{51}$
2950	$120.3^{+25.8}_{-32.0}$	$8.18^{+14.36}_{-4.92}$	$(2.86^{+24.88}_{-2.53}) \times 10^{53}$
2951	$148.6^{+51.9}_{-63.1}$	$6.52^{+25.25}_{-4.74}$	$(2.93^{+98.27}_{-2.80}) \times 10^{53}$
2953	$196.3^{+5.2}_{-5.0}$	$1.11^{+0.04}_{-0.04}$	$(4.03^{+0.39}_{-0.35}) \times 10^{52}$
2958	$144.6^{+17.0}_{-14.7}$	$2.87^{+0.84}_{-0.57}$	$(7.35^{+6.27}_{-3.03}) \times 10^{52}$
2988	$199.1^{+34.3}_{-28.5}$	$7.94^{+9.11}_{-3.19}$	$(7.44^{+34.23}_{-5.18}) \times 10^{53}$
2998	$72.8^{+5.3}_{-7.8}$	$3.03^{+0.54}_{-0.64}$	$(2.02^{+0.97}_{-0.88}) \times 10^{52}$
3001	$219.3^{+20.8}_{-19.5}$	$7.40^{+3.36}_{-2.00}$	$(7.96^{+10.75}_{-4.12}) \times 10^{53}$
3003	$326.5^{+13.9}_{-13.1}$	$7.40^{+1.31}_{-1.00}$	$(1.77^{+0.80}_{-0.50}) \times 10^{54}$
3011	$178.4^{+42.7}_{-39.6}$	$1.77^{+0.88}_{-0.58}$	$(5.73^{+9.53}_{-3.56}) \times 10^{52}$
3012	$76.8^{+42.0}_{-28.1}$	$2.24^{+4.55}_{-1.17}$	$(1.45^{+18.67}_{-1.21}) \times 10^{52}$
3015	$170.5^{+29.3}_{-24.1}$	$11.37^{+19.51}_{-5.18}$	$(1.04^{+8.48}_{-0.78}) \times 10^{54}$
3032	$103.1^{+15.1}_{-9.8}$	$3.31^{+1.40}_{-0.65}$	$(4.63^{+6.06}_{-1.90}) \times 10^{52}$
3035	$167.1^{+76.6}_{-47.2}$	$1.04^{+0.82}_{-0.37}$	$(2.73^{+8.70}_{-1.78}) \times 10^{52}$
3039	$132.9^{+6.4}_{-6.3}$	$1.83^{+0.16}_{-0.14}$	$(3.31^{+0.75}_{-0.60}) \times 10^{52}$
3042	$303.1^{+14.1}_{-13.3}$	$2.99^{+0.33}_{-0.28}$	$(3.44^{+0.97}_{-0.72}) \times 10^{53}$
3055	$73.4^{+1.9}_{-2.7}$	$1.75^{+0.08}_{-0.11}$	$(9.57^{+1.08}_{-1.35}) \times 10^{51}$
3056	$125.9^{+16.8}_{-13.7}$	$2.34^{+0.70}_{-0.45}$	$(4.16^{+3.65}_{-1.68}) \times 10^{52}$
3057	$683.9^{+14.4}_{-13.9}$	$1.28^{+0.04}_{-0.04}$	$(5.71^{+0.46}_{-0.41}) \times 10^{53}$
3067	$380.4^{+12.5}_{-11.8}$	$1.88^{+0.11}_{-0.10}$	$(2.82^{+0.42}_{-0.36}) \times 10^{53}$
3068	$132.4^{+26.2}_{-38.5}$	$9.63^{+17.80}_{-6.34}$	$(4.65^{+43.07}_{-4.27}) \times 10^{53}$
3070	$171.2^{+23.7}_{-33.5}$	$11.00^{+12.34}_{-6.06}$	$(9.91^{+42.96}_{-8.34}) \times 10^{53}$
3072	$55.5^{+16.4}_{-31.2}$	$2.04^{+1.47}_{-1.42}$	$(6.66^{+17.94}_{-6.30}) \times 10^{51}$
3075	$49.7^{+31.5}_{-37.5}$	$1.67^{+3.10}_{-1.39}$	$(4.13^{+47.39}_{-4.08}) \times 10^{51}$
3076	$93.0^{+38.5}_{-38.2}$	$3.36^{+6.75}_{-2.08}$	$(3.85^{+46.14}_{-3.48}) \times 10^{52}$
3084	$166.6^{+35.3}_{-37.0}$	$6.57^{+8.70}_{-3.32}$	$(3.73^{+21.55}_{-3.02}) \times 10^{53}$
3085	$91.3^{+24.4}_{-40.9}$	$6.04^{+11.13}_{-4.44}$	$(9.70^{+94.06}_{-9.29}) \times 10^{52}$
3093	$128.6^{+31.5}_{-36.9}$	$6.45^{+10.93}_{-3.80}$	$(2.15^{+18.15}_{-1.89}) \times 10^{53}$
3096	$240.9^{+34.7}_{-47.8}$	$10.99^{+13.12}_{-6.10}$	$(1.96^{+9.27}_{-1.65}) \times 10^{54}$
3100	$54.2^{+2.0}_{-1.2}$	$1.88^{+0.13}_{-0.07}$	$(5.73^{+0.98}_{-0.51}) \times 10^{51}$
3101	$107.5^{+5.4}_{-5.5}$	$1.69^{+0.15}_{-0.14}$	$(1.96^{+0.44}_{-0.38}) \times 10^{52}$
3105	$259.7^{+8.3}_{-7.5}$	$8.91^{+1.30}_{-0.98}$	$(1.55^{+0.56}_{-0.36}) \times 10^{54}$
3109	$111.1^{+12.0}_{-10.8}$	$7.66^{+4.24}_{-2.25}$	$(2.17^{+3.74}_{-1.20}) \times 10^{53}$

TABLE 2—*Continued*

Trigger Number	E_p (keV)	Redshift	Luminosity (ergs s^{-1})
3115	$310.8^{+7.0}_{-6.8}$	$3.72^{+0.22}_{-0.20}$	$(5.04^{+0.73}_{-0.61}) \times 10^{53}$
3119	$52.4^{+13.8}_{-14.8}$	$1.46^{+0.72}_{-0.55}$	$(3.88^{+6.49}_{-2.68}) \times 10^{51}$
3120	$108.8^{+46.7}_{-41.4}$	$4.47^{+15.08}_{-2.83}$	$(8.32^{+231.45}_{-7.57}) \times 10^{52}$
3128	$382.1^{+7.1}_{-6.9}$	$2.80^{+0.11}_{-0.11}$	$(4.94^{+0.50}_{-0.44}) \times 10^{53}$
3129	$72.5^{+9.8}_{-12.3}$	$2.26^{+0.67}_{-0.63}$	$(1.31^{+1.15}_{-0.72}) \times 10^{52}$
3131	$40.0^{+1.0}_{-2.2}$	$0.80^{+0.03}_{-0.06}$	$(1.22^{+0.10}_{-0.20}) \times 10^{51}$
3132	$81.5^{+4.0}_{-4.3}$	$4.72^{+0.73}_{-0.65}$	$(5.11^{+2.04}_{-1.51}) \times 10^{52}$
3138	$217.6^{+6.5}_{-6.2}$	$1.33^{+0.06}_{-0.06}$	$(6.00^{+0.70}_{-0.62}) \times 10^{52}$
3142	$248.9^{+45.9}_{-61.7}$	$9.33^{+14.42}_{-5.60}$	$(1.55^{+10.94}_{-1.37}) \times 10^{54}$
3143	$130.6^{+43.4}_{-35.4}$	$1.65^{+1.17}_{-0.62}$	$(2.80^{+7.55}_{-1.93}) \times 10^{52}$
3153	$28.8^{+11.9}_{-14.1}$	$0.83^{+0.52}_{-0.46}$	$(6.55^{+14.94}_{-5.59}) \times 10^{50}$
3159	$43.3^{+31.5}_{-38.6}$	$1.28^{+2.23}_{-1.17}$	$(2.29^{+24.45}_{-2.28}) \times 10^{51}$
3166	$41.4^{+43.9}_{-25.4}$	$1.23^{+4.11}_{-0.86}$	$(2.00^{+66.64}_{-1.89}) \times 10^{51}$
3177	$197.8^{+29.4}_{-24.5}$	$8.75^{+8.72}_{-3.29}$	$(8.72^{+32.60}_{-5.78}) \times 10^{53}$
3193	$121.7^{+34.1}_{-28.8}$	$7.81^{+23.20}_{-4.34}$	$(2.70^{+55.61}_{-2.29}) \times 10^{53}$
3212	$105.8^{+36.8}_{-51.1}$	$1.38^{+0.92}_{-0.81}$	$(1.49^{+3.72}_{-1.32}) \times 10^{52}$
3217	$51.6^{+47.5}_{-16.7}$	$0.85^{+1.50}_{-0.33}$	$(2.14^{+23.69}_{-1.48}) \times 10^{51}$
3220	$78.8^{+22.5}_{-18.5}$	$2.70^{+2.33}_{-1.06}$	$(2.00^{+6.77}_{-1.40}) \times 10^{52}$
3227	$222.2^{+10.6}_{-10.2}$	$1.67^{+0.14}_{-0.12}$	$(8.25^{+1.76}_{-1.43}) \times 10^{52}$
3237	$97.3^{+14.9}_{-20.4}$	$1.34^{+0.34}_{-0.38}$	$(1.22^{+0.90}_{-0.68}) \times 10^{52}$
3238	$95.4^{+67.2}_{-51.2}$	$1.54^{+3.12}_{-0.99}$	$(1.38^{+18.53}_{-1.27}) \times 10^{52}$
3241	$297.2^{+10.1}_{-9.9}$	$3.05^{+0.24}_{-0.22}$	$(3.41^{+0.69}_{-0.56}) \times 10^{53}$
3242	$23.6^{+13.2}_{-7.7}$	$0.34^{+0.22}_{-0.12}$	$(2.34^{+5.41}_{-1.46}) \times 10^{50}$
3245	$342.9^{+13.4}_{-11.6}$	$2.20^{+0.17}_{-0.14}$	$(2.83^{+0.56}_{-0.41}) \times 10^{53}$
3246	$119.5^{+17.9}_{-36.9}$	$10.67^{+13.24}_{-7.40}$	$(4.56^{+22.91}_{-4.27}) \times 10^{53}$
3247	$211.7^{+59.6}_{-77.0}$	$6.47^{+14.59}_{-4.35}$	$(5.86^{+78.13}_{-5.45}) \times 10^{53}$
3255	$91.4^{+12.5}_{-11.6}$	$0.69^{+0.12}_{-0.10}$	$(5.58^{+2.69}_{-1.85}) \times 10^{51}$
3256	$141.8^{+6.1}_{-6.6}$	$3.42^{+0.38}_{-0.36}$	$(9.23^{+2.60}_{-2.15}) \times 10^{52}$
3257	$210.5^{+6.3}_{-5.9}$	$11.97^{+1.98}_{-1.52}$	$(1.75^{+0.72}_{-0.46}) \times 10^{54}$
3259	$265.4^{+68.7}_{-48.1}$	$8.96^{+27.42}_{-4.41}$	$(1.64^{+34.96}_{-1.30}) \times 10^{54}$
3279	$76.3^{+17.6}_{-17.6}$	$2.95^{+2.05}_{-1.17}$	$(2.13^{+5.32}_{-1.50}) \times 10^{52}$
3283	$185.8^{+32.0}_{-29.4}$	$10.61^{+16.86}_{-5.07}$	$(1.09^{+7.93}_{-0.85}) \times 10^{54}$
3287	$198.1^{+15.0}_{-13.9}$	$4.00^{+0.89}_{-0.66}$	$(2.31^{+1.39}_{-0.81}) \times 10^{53}$
3290	$144.3^{+5.2}_{-5.1}$	$1.06^{+0.05}_{-0.05}$	$(2.06^{+0.27}_{-0.24}) \times 10^{52}$
3292	$97.3^{+38.0}_{-43.4}$	$5.81^{+24.78}_{-4.23}$	$(1.03^{+41.83}_{-0.99}) \times 10^{53}$
3306	$130.8^{+24.5}_{-22.6}$	$2.80^{+1.42}_{-0.86}$	$(5.79^{+9.61}_{-3.43}) \times 10^{52}$
3307	$46.1^{+26.3}_{-20.5}$	$1.56^{+2.26}_{-0.87}$	$(3.27^{+25.29}_{-2.83}) \times 10^{51}$
3319	$207.2^{+36.6}_{-38.2}$	$9.03^{+12.42}_{-4.50}$	$(1.01^{+6.02}_{-0.81}) \times 10^{54}$
3320	$115.5^{+17.6}_{-10.5}$	$6.36^{+4.86}_{-1.64}$	$(1.70^{+4.51}_{-0.85}) \times 10^{53}$
3330	$434.3^{+25.4}_{-23.3}$	$5.16^{+1.02}_{-0.76}$	$(1.68^{+0.88}_{-0.52}) \times 10^{54}$
3336	$104.3^{+41.5}_{-37.7}$	$2.84^{+4.33}_{-1.55}$	$(3.77^{+29.61}_{-3.22}) \times 10^{52}$
3345	$201.5^{+12.3}_{-10.8}$	$1.70^{+0.18}_{-0.15}$	$(6.95^{+1.98}_{-1.38}) \times 10^{52}$
3351	$159.3^{+45.7}_{-45.0}$	$4.29^{+5.95}_{-2.23}$	$(1.67^{+10.80}_{-1.38}) \times 10^{53}$
3352	$149.1^{+9.6}_{-8.2}$	$1.87^{+0.22}_{-0.17}$	$(4.30^{+1.35}_{-0.91}) \times 10^{52}$
3356	$100.5^{+25.3}_{-26.1}$	$2.62^{+1.84}_{-1.10}$	$(3.10^{+7.96}_{-2.27}) \times 10^{52}$
3364	$105.1^{+12.4}_{-17.3}$	$8.91^{+6.33}_{-4.11}$	$(2.54^{+5.98}_{-1.93}) \times 10^{53}$
3369	$83.7^{+22.7}_{-14.0}$	$3.99^{+4.66}_{-1.38}$	$(4.09^{+20.64}_{-2.61}) \times 10^{52}$
3370	$41.9^{+35.8}_{-31.4}$	$1.16^{+2.41}_{-0.94}$	$(1.92^{+27.68}_{-1.89}) \times 10^{51}$
3403	$87.1^{+17.1}_{-34.2}$	$6.43^{+7.31}_{-4.48}$	$(9.82^{+45.51}_{-9.25}) \times 10^{52}$
3407	$112.5^{+58.7}_{-52.8}$	$4.09^{+20.06}_{-2.87}$	$(7.69^{+427.25}_{-7.27}) \times 10^{52}$
3408	$348.7^{+6.3}_{-6.3}$	$3.73^{+0.17}_{-0.16}$	$(6.39^{+0.73}_{-0.65}) \times 10^{53}$
3415	$205.9^{+7.0}_{-6.8}$	$2.44^{+0.17}_{-0.15}$	$(1.18^{+0.21}_{-0.17}) \times 10^{53}$
3436	$193.0^{+15.7}_{-14.9}$	$8.85^{+3.81}_{-2.31}$	$(8.48^{+10.60}_{-4.24}) \times 10^{53}$
3448	$176.1^{+72.8}_{-56.8}$	$3.00^{+5.20}_{-1.53}$	$(1.16^{+11.13}_{-0.96}) \times 10^{53}$
3458	$236.7^{+8.2}_{-7.9}$	$2.14^{+0.14}_{-0.13}$	$(1.30^{+0.22}_{-0.18}) \times 10^{53}$
3480	$370.8^{+10.0}_{-9.6}$	$2.82^{+0.17}_{-0.15}$	$(4.71^{+0.70}_{-0.59}) \times 10^{53}$
3481	$395.5^{+10.4}_{-10.1}$	$1.79^{+0.08}_{-0.08}$	$(2.85^{+0.33}_{-0.29}) \times 10^{53}$
3485	$113.2^{+19.6}_{-17.7}$	$10.61^{+16.98}_{-5.02}$	$(4.05^{+29.76}_{-3.12}) \times 10^{53}$
3488	$321.8^{+32.3}_{-28.9}$	$5.28^{+1.99}_{-1.23}$	$(9.57^{+10.51}_{-4.45}) \times 10^{53}$
3489	$327.7^{+10.4}_{-10.0}$	$6.81^{+0.83}_{-0.69}$	$(1.54^{+0.47}_{-0.34}) \times 10^{54}$
3491	$221.8^{+13.3}_{-12.4}$	$0.90^{+0.07}_{-0.07}$	$(4.19^{+0.88}_{-0.71}) \times 10^{52}$
3503	$106.1^{+19.3}_{-22.6}$	$10.57^{+18.64}_{-6.03}$	$(3.54^{+30.18}_{-3.04}) \times 10^{53}$
3511	$45.0^{+13.2}_{-19.7}$	$1.39^{+0.76}_{-0.76}$	$(2.72^{+5.18}_{-2.32}) \times 10^{51}$
3512	$223.2^{+13.6}_{-12.4}$	$2.36^{+0.30}_{-0.24}$	$(1.32^{+0.44}_{-0.31}) \times 10^{53}$
3514	$128.6^{+33.5}_{-42.5}$	$5.49^{+8.53}_{-3.36}$	$(1.63^{+12.26}_{-1.46}) \times 10^{53}$

TABLE 2—*Continued*

Trigger Number	E_p (keV)	Redshift	Luminosity (ergs s^{-1})
3516	$261.3^{+40.7}_{-37.0}$	$10.12^{+12.66}_{-4.42}$	$(1.98^{+10.12}_{-1.45}) \times 10^{54}$
3523	$642.5^{+8.6}_{-8.5}$	$1.58^{+0.03}_{-0.03}$	$(6.46^{+0.36}_{-0.34}) \times 10^{53}$
3527	$215.1^{+54.4}_{-50.9}$	$9.69^{+31.81}_{-5.73}$	$(1.24^{+29.53}_{-1.08}) \times 10^{54}$
3567	$108.6^{+21.7}_{-9.1}$	$6.55^{+7.85}_{-1.59}$	$(1.58^{+7.89}_{-0.75}) \times 10^{53}$
3569	$216.1^{+47.8}_{-36.6}$	$3.11^{+2.13}_{-0.98}$	$(1.85^{+4.52}_{-1.11}) \times 10^{53}$
3588	$60.2^{+28.2}_{-31.9}$	$1.24^{+1.12}_{-0.77}$	$(4.27^{+16.47}_{-3.86}) \times 10^{51}$
3598	$235.5^{+17.5}_{-16.2}$	$6.77^{+2.13}_{-1.41}$	$(7.85^{+6.86}_{-3.29}) \times 10^{53}$
3608	$44.8^{+24.9}_{-27.4}$	$0.61^{+0.47}_{-0.40}$	$(1.22^{+3.73}_{-1.12}) \times 10^{51}$
3618	$252.9^{+12.9}_{-12.3}$	$7.18^{+1.52}_{-1.14}$	$(1.00^{+0.55}_{-0.33}) \times 10^{54}$
3634	$254.8^{+40.1}_{-34.3}$	$6.83^{+5.83}_{-2.47}$	$(9.35^{+28.76}_{-6.07}) \times 10^{53}$
3637	$164.9^{+11.2}_{-10.1}$	$7.49^{+2.29}_{-1.49}$	$(4.60^{+3.86}_{-1.85}) \times 10^{53}$
3648	$199.0^{+7.4}_{-7.2}$	$3.88^{+0.39}_{-0.34}$	$(2.21^{+0.57}_{-0.43}) \times 10^{53}$
3649	$239.7^{+21.0}_{-20.1}$	$6.28^{+2.28}_{-1.50}$	$(7.14^{+7.42}_{-3.36}) \times 10^{53}$
3658	$247.2^{+5.9}_{-5.7}$	$1.65^{+0.07}_{-0.06}$	$(1.00^{+0.10}_{-0.09}) \times 10^{53}$
3662	$224.0^{+15.6}_{-13.6}$	$1.91^{+0.25}_{-0.20}$	$(9.96^{+3.47}_{-2.31}) \times 10^{52}$
3663	$197.2^{+22.1}_{-19.1}$	$2.86^{+0.80}_{-0.54}$	$(1.36^{+1.09}_{-0.54}) \times 10^{53}$
3664	$79.4^{+6.2}_{-4.4}$	$2.37^{+0.39}_{-0.24}$	$(1.67^{+0.75}_{-0.39}) \times 10^{52}$
3765	$298.1^{+5.7}_{-5.6}$	$1.27^{+0.04}_{-0.04}$	$(1.08^{+0.08}_{-0.07}) \times 10^{53}$
3776	$180.0^{+7.6}_{-6.9}$	$2.50^{+0.22}_{-0.18}$	$(9.31^{+2.14}_{-1.58}) \times 10^{52}$
3788	$204.8^{+5.7}_{-5.5}$	$2.14^{+0.11}_{-0.10}$	$(9.70^{+1.31}_{-1.12}) \times 10^{52}$
3811	$55.6^{+1.8}_{-2.1}$	$1.22^{+0.06}_{-0.07}$	$(3.58^{+0.44}_{-0.46}) \times 10^{51}$
3815	$46.3^{+11.8}_{-11.3}$	$0.87^{+0.32}_{-0.26}$	$(1.77^{+2.06}_{-1.02}) \times 10^{51}$
3843	$193.6^{+10.1}_{-29.4}$	$7.56^{+1.69}_{-3.10}$	$(6.45^{+3.79}_{-4.56}) \times 10^{53}$
3866	$310.7^{+61.4}_{-41.3}$	$10.15^{+20.01}_{-4.25}$	$(2.81^{+28.71}_{-2.00}) \times 10^{54}$
3869	$77.7^{+41.5}_{-47.3}$	$1.63^{+2.22}_{-1.16}$	$(9.76^{+68.37}_{-9.29}) \times 10^{51}$
3870	$135.8^{+30.6}_{-19.2}$	$0.66^{+0.19}_{-0.11}$	$(1.19^{+1.04}_{-0.42}) \times 10^{52}$
3875	$77.3^{+4.6}_{-4.8}$	$1.48^{+0.15}_{-0.14}$	$(8.60^{+2.24}_{-1.88}) \times 10^{51}$
3879	$95.6^{+16.2}_{-18.3}$	$2.75^{+1.21}_{-0.91}$	$(3.01^{+4.20}_{-1.89}) \times 10^{52}$
3886	$160.4^{+44.7}_{-33.7}$	$5.81^{+11.06}_{-2.72}$	$(2.80^{+28.73}_{-2.17}) \times 10^{53}$
3890	$104.2^{+19.9}_{-20.5}$	$10.72^{+21.12}_{-5.87}$	$(3.50^{+35.48}_{-2.94}) \times 10^{53}$
3891	$216.2^{+11.4}_{-10.5}$	$1.25^{+0.10}_{-0.09}$	$(5.57^{+1.16}_{-0.91}) \times 10^{52}$
3892	$32.4^{+31.4}_{-18.4}$	$0.58^{+0.86}_{-0.35}$	$(6.13^{+50.79}_{-5.44}) \times 10^{50}$
3893	$168.7^{+3.8}_{-3.7}$	$4.53^{+0.29}_{-0.27}$	$(2.05^{+0.33}_{-0.28}) \times 10^{53}$
3900	$87.8^{+116.0}_{-317.4}$	$1.11^{+5.13}_{8.75}$	$(8.09^{+503.70}_{1450.37}) \times 10^{51}$
3905	$228.8^{+15.6}_{-14.3}$	$3.77^{+0.72}_{-0.54}$	$(2.80^{+1.43}_{-0.87}) \times 10^{53}$
3906	$120.3^{+9.9}_{-9.2}$	$3.73^{+0.87}_{-0.64}$	$(7.59^{+4.90}_{-2.76}) \times 10^{52}$
3909	$58.2^{+26.9}_{-25.3}$	$1.03^{+0.82}_{-0.53}$	$(3.29^{+10.54}_{-2.71}) \times 10^{51}$
3912	$198.0^{+17.6}_{-16.2}$	$4.39^{+1.25}_{-0.87}$	$(2.67^{+2.14}_{-1.09}) \times 10^{53}$
3916	$101.8^{+28.5}_{-26.8}$	$5.00^{+7.95}_{-2.59}$	$(8.74^{+68.74}_{-7.21}) \times 10^{52}$
3918	$273.7^{+19.2}_{-17.5}$	$7.99^{+2.65}_{-1.70}$	$(1.42^{+1.31}_{-0.60}) \times 10^{54}$
3929	$274.9^{+12.0}_{-11.2}$	$4.13^{+0.51}_{-0.42}$	$(4.67^{+1.49}_{-1.05}) \times 10^{53}$
3930	$512.1^{+12.3}_{-11.9}$	$5.61^{+0.44}_{-0.39}$	$(2.69^{+0.52}_{-0.42}) \times 10^{54}$
3936	$182.9^{+6.5}_{-6.2}$	$2.78^{+0.22}_{-0.19}$	$(1.12^{+0.23}_{-0.18}) \times 10^{53}$
3954	$304.9^{+13.9}_{-13.4}$	$2.40^{+0.23}_{-0.20}$	$(2.51^{+0.62}_{-0.48}) \times 10^{53}$
4048	$355.9^{+20.1}_{-18.6}$	$6.95^{+1.62}_{-1.15}$	$(1.88^{+1.16}_{-0.65}) \times 10^{54}$
4157	$85.3^{+6.4}_{-5.0}$	$2.37^{+0.38}_{-0.26}$	$(1.94^{+0.83}_{-0.48}) \times 10^{52}$
4216	$56.9^{+10.9}_{-15.7}$	$0.90^{+0.25}_{-0.30}$	$(2.75^{+2.23}_{-1.73}) \times 10^{51}$
4312	$109.6^{+10.4}_{-10.1}$	$0.98^{+0.13}_{-0.12}$	$(1.11^{+0.40}_{-0.30}) \times 10^{52}$
4350	$85.2^{+27.9}_{-19.6}$	$1.05^{+0.55}_{-0.30}$	$(7.13^{+13.15}_{-4.06}) \times 10^{51}$
4556	$264.1^{+6.6}_{-6.1}$	$1.55^{+0.06}_{-0.06}$	$(1.07^{+0.11}_{-0.09}) \times 10^{53}$
4701	$238.2^{+8.1}_{-7.8}$	$3.76^{+0.34}_{-0.30}$	$(3.02^{+0.68}_{-0.54}) \times 10^{53}$
4710	$99.0^{+5.0}_{-5.3}$	$1.02^{+0.07}_{-0.07}$	$(9.33^{+1.72}_{-1.59}) \times 10^{51}$
4814	$217.4^{+28.3}_{-37.2}$	$7.76^{+5.63}_{-3.49}$	$(8.51^{+20.83}_{-6.40}) \times 10^{53}$
5080	$43.2^{+2.7}_{-2.3}$	$0.89^{+0.08}_{-0.06}$	$(1.57^{+0.35}_{-0.25}) \times 10^{51}$
5304	$471.7^{+17.9}_{-17.0}$	$3.33^{+0.31}_{-0.27}$	$(9.77^{+2.34}_{-1.79}) \times 10^{53}$
5389	$182.7^{+8.5}_{-8.0}$	$3.95^{+0.51}_{-0.42}$	$(1.92^{+0.64}_{-0.45}) \times 10^{53}$
5415	$125.3^{+13.6}_{-11.3}$	$7.16^{+3.77}_{-1.92}$	$(2.45^{+3.99}_{-1.27}) \times 10^{53}$
5416	$117.2^{+17.7}_{-16.4}$	$10.91^{+13.97}_{-4.86}$	$(4.57^{+24.02}_{-3.38}) \times 10^{53}$
5417	$176.6^{+9.6}_{-8.9}$	$1.35^{+0.11}_{-0.10}$	$(4.05^{+0.90}_{-0.71}) \times 10^{52}$
5419	$97.2^{+52.8}_{-30.3}$	$1.56^{+2.09}_{-0.65}$	$(1.45^{+9.93}_{-1.07}) \times 10^{52}$
5428	$73.5^{+6.9}_{-14.6}$	$2.67^{+0.58}_{-0.91}$	$(1.70^{+1.03}_{-1.08}) \times 10^{52}$
5429	$78.1^{+21.6}_{-29.7}$	$1.12^{+0.51}_{-0.52}$	$(6.45^{+9.68}_{-5.04}) \times 10^{51}$
5433	$194.6^{+14.9}_{-14.1}$	$6.78^{+2.21}_{-1.48}$	$(5.38^{+4.89}_{-2.34}) \times 10^{53}$
5434	$97.9^{+28.3}_{-29.0}$	$8.66^{+33.64}_{-5.60}$	$(2.10^{+68.06}_{-1.92}) \times 10^{53}$
5439	$266.0^{+45.5}_{-34.0}$	$4.66^{+3.18}_{-1.38}$	$(5.32^{+12.46}_{-3.01}) \times 10^{53}$

TABLE 2—*Continued*

Trigger Number	E_p (keV)	Redshift	Luminosity (ergs s^{-1})
5447	$37.9^{+18.6}_{-2.6}$	$0.51^{+0.32}_{-0.04}$	$(7.70^{+17.50}_{-1.36}) \times 10^{50}$
5451	$193.1^{+7.6}_{-7.3}$	$5.10^{+0.65}_{-0.54}$	$(3.25^{+1.05}_{-0.75}) \times 10^{53}$
5463	$103.0^{+10.1}_{-25.5}$	$8.68^{+4.71}_{-5.10}$	$(2.33^{+3.89}_{-2.04}) \times 10^{53}$
5472	$133.6^{+26.6}_{-23.1}$	$6.23^{+7.01}_{-2.61}$	$(2.19^{+10.03}_{-1.58}) \times 10^{53}$
5474	$37.4^{+2.7}_{-2.9}$	$1.21^{+0.13}_{-0.13}$	$(1.60^{+0.47}_{-0.39}) \times 10^{51}$
5476	$167.4^{+30.5}_{-26.2}$	$6.60^{+6.83}_{-2.63}$	$(3.80^{+15.32}_{-2.64}) \times 10^{53}$
5477	$1456.8^{+73.8}_{-50.2}$	$5.46^{+0.95}_{-0.55}$	$(2.08^{+0.94}_{-0.46}) \times 10^{55}$
5478	$178.2^{+9.9}_{-10.3}$	$5.81^{+1.17}_{-0.97}$	$(3.45^{+1.83}_{-1.20}) \times 10^{53}$
5479	$170.8^{+23.3}_{-21.2}$	$3.86^{+1.68}_{-1.03}$	$(1.62^{+2.17}_{-0.85}) \times 10^{53}$
5486	$262.4^{+8.4}_{-8.0}$	$2.20^{+0.14}_{-0.12}$	$(1.66^{+0.26}_{-0.22}) \times 10^{53}$
5489	$312.0^{+8.2}_{-8.0}$	$3.62^{+0.24}_{-0.22}$	$(4.88^{+0.82}_{-0.68}) \times 10^{53}$
5493	$91.6^{+40.2}_{-45.7}$	$5.53^{+30.71}_{-4.22}$	$(8.40^{+556.70}_{-8.13}) \times 10^{52}$
5504	$91.7^{+44.8}_{-33.5}$	$1.82^{+2.41}_{-0.90}$	$(1.57^{+10.39}_{-1.27}) \times 10^{52}$
5508	$76.2^{+11.9}_{-11.4}$	$3.96^{+2.10}_{-1.24}$	$(3.35^{+5.72}_{-1.99}) \times 10^{52}$
5515	$91.8^{+63.6}_{-50.5}$	$2.57^{+10.82}_{-1.82}$	$(2.52^{+114.74}_{-2.39}) \times 10^{52}$
5517	$138.7^{+31.5}_{-24.8}$	$3.31^{+2.47}_{-1.12}$	$(8.37^{+22.87}_{-5.27}) \times 10^{52}$
5518	$163.3^{+15.6}_{-13.9}$	$5.54^{+2.03}_{-1.26}$	$(2.67^{+2.84}_{-1.22}) \times 10^{53}$
5523	$135.2^{+21.5}_{-20.2}$	$2.26^{+0.81}_{-0.57}$	$(4.57^{+4.99}_{-2.32}) \times 10^{52}$
5530	$71.3^{+5.8}_{-5.6}$	$1.09^{+0.13}_{-0.12}$	$(5.23^{+1.67}_{-1.27}) \times 10^{51}$
5531	$131.9^{+16.9}_{-16.2}$	$5.99^{+3.41}_{-1.91}$	$(1.99^{+3.63}_{-1.18}) \times 10^{53}$
5539	$112.2^{+15.7}_{-18.0}$	$4.73^{+2.48}_{-1.69}$	$(9.70^{+16.16}_{-6.29}) \times 10^{52}$
5541	$145.7^{+31.2}_{-28.3}$	$9.15^{+18.60}_{-4.74}$	$(5.12^{+55.54}_{-4.18}) \times 10^{53}$
5542	$219.5^{+7.9}_{-7.5}$	$5.63^{+0.69}_{-0.57}$	$(4.97^{+1.54}_{-1.10}) \times 10^{53}$
5548	$165.2^{+20.8}_{-18.1}$	$1.84^{+0.44}_{-0.32}$	$(5.15^{+3.59}_{-1.94}) \times 10^{52}$
5551	$68.1^{+24.4}_{-11.6}$	$2.04^{+1.91}_{-0.56}$	$(1.01^{+3.91}_{-0.54}) \times 10^{52}$
5563	$184.1^{+10.5}_{-9.9}$	$1.16^{+0.10}_{-0.09}$	$(3.72^{+0.82}_{-0.65}) \times 10^{52}$
5567	$359.8^{+8.5}_{-8.3}$	$1.86^{+0.08}_{-0.07}$	$(2.48^{+0.26}_{-0.23}) \times 10^{53}$
5568	$509.3^{+19.6}_{-18.5}$	$2.71^{+0.23}_{-0.20}$	$(8.38^{+1.81}_{-1.42}) \times 10^{53}$
5571	$147.0^{+62.6}_{-49.2}$	$3.02^{+5.60}_{-1.59}$	$(8.19^{+87.14}_{-6.87}) \times 10^{52}$
5572	$189.6^{+18.3}_{-20.4}$	$2.95^{+0.71}_{-0.62}$	$(1.31^{+0.88}_{-0.57}) \times 10^{53}$
5575	$215.6^{+16.9}_{-16.0}$	$2.94^{+0.56}_{-0.44}$	$(1.69^{+0.87}_{-0.55}) \times 10^{53}$
5585	$153.2^{+29.1}_{-38.1}$	$7.00^{+8.27}_{-3.88}$	$(3.52^{+17.13}_{-2.99}) \times 10^{53}$
5593	$228.3^{+8.6}_{-8.1}$	$7.28^{+1.10}_{-0.88}$	$(8.37^{+3.20}_{-2.15}) \times 10^{53}$
5601	$279.8^{+57.1}_{-46.6}$	$5.00^{+4.69}_{-1.87}$	$(6.61^{+23.81}_{-4.44}) \times 10^{53}$
5603	$160.5^{+28.1}_{-25.7}$	$11.64^{+21.30}_{-5.78}$	$(9.65^{+86.42}_{-7.65}) \times 10^{53}$
5604	$273.6^{+22.7}_{-19.8}$	$6.07^{+2.01}_{-1.26}$	$(8.79^{+8.22}_{-3.68}) \times 10^{53}$
5606	$165.4^{+22.9}_{-36.2}$	$6.40^{+4.28}_{-3.18}$	$(3.51^{+7.84}_{-2.82}) \times 10^{53}$
5608	$202.9^{+20.7}_{-33.4}$	$8.10^{+4.36}_{-3.61}$	$(8.00^{+13.26}_{-5.97}) \times 10^{53}$
5621	$259.1^{+8.6}_{-8.1}$	$1.07^{+0.05}_{-0.05}$	$(6.74^{+0.80}_{-0.71}) \times 10^{52}$
5624	$226.4^{+49.5}_{-44.2}$	$8.18^{+14.98}_{-4.10}$	$(1.01^{+9.41}_{-0.81}) \times 10^{54}$
5628	$237.4^{+12.6}_{-12.0}$	$2.71^{+0.32}_{-0.27}$	$(1.82^{+0.57}_{-0.41}) \times 10^{53}$
5637	$154.4^{+82.1}_{-47.9}$	$4.53^{+29.95}_{-2.54}$	$(1.71^{+163.40}_{-1.47}) \times 10^{53}$
5640	$69.7^{+11.0}_{-10.0}$	$3.82^{+1.96}_{-1.14}$	$(2.65^{+4.38}_{-1.52}) \times 10^{52}$
5644	$301.9^{+16.2}_{-14.9}$	$3.32^{+0.45}_{-0.36}$	$(3.98^{+1.41}_{-0.96}) \times 10^{53}$
5645	$101.3^{+36.2}_{-50.6}$	$3.38^{+5.20}_{-2.36}$	$(4.62^{+36.04}_{-4.37}) \times 10^{52}$
5654	$255.1^{+4.7}_{-4.6}$	$3.98^{+0.20}_{-0.18}$	$(3.79^{+0.46}_{-0.40}) \times 10^{53}$
5655	$74.3^{+41.8}_{-32.8}$	$2.87^{+8.85}_{-1.81}$	$(1.94^{+49.25}_{-1.77}) \times 10^{52}$
5667	$136.4^{+45.5}_{-29.3}$	$4.02^{+6.74}_{-1.68}$	$(1.10^{+9.63}_{-0.80}) \times 10^{53}$
5697	$50.4^{+6.8}_{-6.6}$	$0.34^{+0.05}_{-0.05}$	$(1.07^{+0.42}_{-0.32}) \times 10^{51}$
5704	$175.5^{+8.2}_{-7.7}$	$1.01^{+0.07}_{-0.06}$	$(2.91^{+0.48}_{-0.41}) \times 10^{52}$
5706	$155.6^{+51.6}_{-74.3}$	$5.32^{+12.92}_{-3.94}$	$(2.27^{+35.00}_{-2.18}) \times 10^{53}$
5711	$487.4^{+18.4}_{-17.6}$	$1.95^{+0.14}_{-0.12}$	$(4.85^{+0.87}_{-0.71}) \times 10^{53}$
5713	$41.0^{+20.1}_{-13.8}$	$1.24^{+1.19}_{-0.53}$	$(1.98^{+8.35}_{-1.48}) \times 10^{51}$
5719	$186.5^{+45.8}_{-38.3}$	$7.80^{+17.10}_{-3.97}$	$(6.32^{+78.61}_{-5.11}) \times 10^{53}$
5726	$113.7^{+8.5}_{-8.1}$	$1.51^{+0.19}_{-0.16}$	$(1.90^{+0.64}_{-0.47}) \times 10^{52}$
5729	$86.0^{+14.5}_{-8.3}$	$1.55^{+0.47}_{-0.23}$	$(1.13^{+1.03}_{-0.36}) \times 10^{52}$
5731	$175.8^{+36.9}_{-20.7}$	$6.33^{+7.92}_{-2.00}$	$(3.90^{+20.79}_{-2.29}) \times 10^{53}$
5773	$182.9^{+1.7}_{-1.7}$	$1.05^{+0.01}_{-0.01}$	$(3.30^{+0.11}_{-0.10}) \times 10^{52}$
5867	$207.1^{+31.0}_{-29.4}$	$8.83^{+9.00}_{-3.67}$	$(9.74^{+37.47}_{-6.92}) \times 10^{53}$
5989	$40.3^{+11.5}_{-10.9}$	$0.15^{+0.05}_{-0.04}$	$(5.07^{+3.96}_{-2.58}) \times 10^{50}$
5995	$706.5^{+8.5}_{-8.3}$	$4.62^{+0.16}_{-0.15}$	$(3.70^{+0.31}_{-0.28}) \times 10^{54}$
6004	$48.1^{+33.3}_{-32.0}$	$1.00^{+1.33}_{-0.73}$	$(2.17^{+15.05}_{-2.07}) \times 10^{51}$
6082	$63.2^{+3.1}_{-9.4}$	$1.79^{+0.16}_{-0.41}$	$(7.28^{+1.64}_{-3.44}) \times 10^{51}$
6083	$100.6^{+7.0}_{-3.8}$	$3.42^{+0.63}_{-0.30}$	$(4.64^{+2.29}_{-0.90}) \times 10^{52}$
6090	$165.7^{+23.8}_{-20.4}$	$3.82^{+1.76}_{-1.01}$	$(1.50^{+2.16}_{-0.78}) \times 10^{53}$

TABLE 2—*Continued*

Trigger Number	E_p (keV)	Redshift	Luminosity (ergs s^{-1})
6098	$113.7^{+19.0}_{-16.4}$	$5.91^{+4.81}_{-2.13}$	$(1.45^{+4.23}_{-0.94}) \times 10^{53}$
6100	$562.1^{+10.9}_{-10.7}$	$3.21^{+0.15}_{-0.14}$	$(1.32^{+0.15}_{-0.13}) \times 10^{54}$
6113	$155.5^{+21.2}_{-18.8}$	$2.12^{+0.61}_{-0.43}$	$(5.53^{+4.69}_{-2.36}) \times 10^{52}$
6124	$405.4^{+7.4}_{-7.3}$	$1.58^{+0.05}_{-0.05}$	$(2.58^{+0.19}_{-0.18}) \times 10^{53}$
6128	$38.4^{+4.4}_{-5.7}$	$0.91^{+0.14}_{-0.17}$	$(1.26^{+0.55}_{-0.51}) \times 10^{51}$
6141	$89.8^{+62.5}_{-38.9}$	$2.14^{+6.58}_{-1.24}$	$(1.86^{+49.49}_{-1.64}) \times 10^{52}$
6147	$85.8^{+3.3}_{-6.3}$	$3.59^{+0.35}_{-0.59}$	$(3.64^{+0.91}_{-1.26}) \times 10^{52}$
6152	$130.0^{+62.3}_{-84.6}$	$4.74^{+24.61}_{-3.99}$	$(1.31^{+78.65}_{-1.29}) \times 10^{53}$
6159	$76.3^{+3.0}_{-13.1}$	$1.74^{+0.12}_{-0.45}$	$(1.02^{+0.18}_{-0.53}) \times 10^{52}$
6167	$59.6^{+11.7}_{-6.5}$	$2.29^{+1.07}_{-0.44}$	$(9.02^{+13.66}_{-3.63}) \times 10^{51}$
6186	$45.0^{+52.8}_{-25.0}$	$0.90^{+2.48}_{-0.56}$	$(1.72^{+41.40}_{-1.55}) \times 10^{51}$
6190	$88.9^{+48.6}_{-27.5}$	$2.48^{+5.70}_{-1.17}$	$(2.24^{+35.08}_{-1.77}) \times 10^{52}$
6194	$136.2^{+19.5}_{-18.4}$	$4.39^{+2.24}_{-1.33}$	$(1.26^{+2.05}_{-0.73}) \times 10^{53}$
6198	$361.4^{+11.5}_{-9.8}$	$0.91^{+0.04}_{-0.03}$	$(1.12^{+0.12}_{-0.10}) \times 10^{53}$
6206	$46.6^{+3.6}_{-3.9}$	$0.90^{+0.10}_{-0.10}$	$(1.84^{+0.51}_{-0.45}) \times 10^{51}$
6216	$108.4^{+15.9}_{-7.4}$	$3.30^{+1.39}_{-0.49}$	$(5.09^{+6.62}_{-1.62}) \times 10^{52}$
6222	$51.9^{+25.1}_{-28.5}$	$1.62^{+1.90}_{-1.07}$	$(4.34^{+24.12}_{-4.03}) \times 10^{51}$
6226	$206.1^{+24.0}_{-38.6}$	$6.74^{+3.73}_{-3.08}$	$(5.98^{+10.39}_{-4.54}) \times 10^{53}$
6235	$388.5^{+11.7}_{-11.2}$	$3.77^{+0.30}_{-0.26}$	$(8.04^{+1.60}_{-1.27}) \times 10^{53}$
6241	$98.9^{+20.3}_{-34.1}$	$1.88^{+0.80}_{-0.89}$	$(1.90^{+2.62}_{-1.51}) \times 10^{52}$
6266	$208.1^{+66.1}_{-70.6}$	$3.14^{+3.68}_{-1.69}$	$(1.74^{+9.03}_{-1.47}) \times 10^{53}$
6272	$61.9^{+1.2}_{-1.4}$	$1.22^{+0.04}_{-0.04}$	$(4.41^{+0.33}_{-0.35}) \times 10^{51}$
6273	$113.5^{+31.6}_{-31.6}$	$5.96^{+11.70}_{-3.37}$	$(1.47^{+15.74}_{-1.26}) \times 10^{53}$
6274	$184.0^{+9.6}_{-8.9}$	$1.11^{+0.08}_{-0.07}$	$(3.52^{+0.69}_{-0.55}) \times 10^{52}$
6280	$121.3^{+24.7}_{-18.3}$	$4.00^{+3.03}_{-1.27}$	$(8.63^{+23.66}_{-5.17}) \times 10^{52}$
6285	$41.4^{+13.6}_{-27.4}$	$1.12^{+0.62}_{-0.82}$	$(1.81^{+3.50}_{-1.73}) \times 10^{51}$
6288	$32.1^{+28.4}_{-3.4}$	$0.54^{+0.69}_{-0.07}$	$(5.72^{+36.85}_{-1.53}) \times 10^{50}$
6295	$84.5^{+7.1}_{-5.9}$	$1.60^{+0.23}_{-0.17}$	$(1.13^{+0.45}_{-0.28}) \times 10^{52}$
6303	$194.1^{+12.2}_{-11.3}$	$4.06^{+0.74}_{-0.57}$	$(2.26^{+1.09}_{-0.68}) \times 10^{53}$
6304	$128.8^{+33.3}_{-48.4}$	$7.01^{+14.70}_{-4.87}$	$(2.49^{+29.27}_{-2.35}) \times 10^{53}$
6309	$33.1^{+43.6}_{-21.9}$	$0.95^{+3.40}_{-0.68}$	$(9.75^{+384.32}_{-9.29}) \times 10^{50}$
6315	$99.0^{+10.4}_{-9.5}$	$2.67^{+0.66}_{-0.48}$	$(3.10^{+2.17}_{-1.19}) \times 10^{52}$
6317	$88.8^{+30.1}_{-39.6}$	$5.85^{+17.28}_{-4.26}$	$(8.68^{+184.54}_{-8.30}) \times 10^{52}$
6319	$113.4^{+36.0}_{-42.4}$	$7.39^{+27.70}_{-5.19}$	$(2.13^{+66.09}_{-2.01}) \times 10^{53}$
6320	$72.7^{+13.8}_{-23.6}$	$1.23^{+0.38}_{-0.50}$	$(6.17^{+5.79}_{-4.48}) \times 10^{51}$
6321	$154.0^{+13.3}_{-12.3}$	$3.02^{+0.65}_{-0.49}$	$(8.98^{+5.31}_{-3.12}) \times 10^{52}$
6322	$83.8^{+21.6}_{-19.6}$	$1.47^{+0.71}_{-0.47}$	$(1.01^{+1.64}_{-0.62}) \times 10^{52}$
6323	$95.3^{+11.1}_{-13.6}$	$5.61^{+2.68}_{-1.96}$	$(9.33^{+13.67}_{-5.93}) \times 10^{52}$
6329	$229.8^{+5.7}_{-5.5}$	$3.16^{+0.18}_{-0.17}$	$(2.14^{+0.31}_{-0.26}) \times 10^{53}$
6335	$147.9^{+13.1}_{-11.7}$	$2.25^{+0.41}_{-0.32}$	$(5.41^{+2.74}_{-1.67}) \times 10^{52}$
6344	$59.1^{+47.0}_{-33.0}$	$1.13^{+2.02}_{-0.72}$	$(3.70^{+41.73}_{-3.39}) \times 10^{51}$
6349	$111.9^{+79.4}_{-54.9}$	$2.16^{+7.11}_{-1.38}$	$(2.94^{+87.81}_{-2.70}) \times 10^{52}$
6351	$45.8^{+5.4}_{-6.5}$	$0.95^{+0.16}_{-0.17}$	$(1.87^{+0.85}_{-0.73}) \times 10^{51}$
6353	$281.4^{+43.0}_{-47.3}$	$10.20^{+12.43}_{-5.00}$	$(2.33^{+11.45}_{-1.83}) \times 10^{54}$
6369	$56.5^{+35.2}_{-29.3}$	$1.80^{+3.52}_{-1.15}$	$(5.85^{+72.83}_{-5.39}) \times 10^{51}$
6397	$198.7^{+5.5}_{-5.3}$	$2.39^{+0.13}_{-0.12}$	$(1.07^{+0.15}_{-0.13}) \times 10^{53}$
6399	$36.5^{+43.4}_{-21.3}$	$0.81^{+2.04}_{-0.52}$	$(1.03^{+21.15}_{-0.93}) \times 10^{51}$
6404	$175.5^{+5.2}_{-5.1}$	$0.96^{+0.04}_{-0.04}$	$(2.77^{+0.28}_{-0.26}) \times 10^{52}$
6405	$85.7^{+28.0}_{-18.1}$	$4.31^{+7.57}_{-1.83}$	$(4.86^{+45.41}_{-3.56}) \times 10^{52}$
6413	$61.0^{+9.6}_{-10.0}$	$0.93^{+0.21}_{-0.19}$	$(3.25^{+2.09}_{-1.41}) \times 10^{51}$
6422	$68.4^{+1.5}_{-1.4}$	$0.70^{+0.02}_{-0.02}$	$(3.17^{+0.22}_{-0.19}) \times 10^{51}$
6436	$156.5^{+47.3}_{-43.4}$	$2.05^{+1.52}_{-0.84}$	$(5.35^{+15.03}_{-3.88}) \times 10^{52}$
6440	$47.7^{+12.5}_{-10.4}$	$0.72^{+0.25}_{-0.18}$	$(1.57^{+1.72}_{-0.80}) \times 10^{51}$
6453	$118.1^{+6.8}_{-6.4}$	$1.61^{+0.16}_{-0.14}$	$(2.22^{+0.58}_{-0.44}) \times 10^{52}$
6472	$470.2^{+46.2}_{-42.2}$	$3.18^{+0.82}_{-0.59}$	$(9.06^{+6.57}_{-3.51}) \times 10^{53}$
6489	$123.9^{+1.4}_{-1.4}$	$3.95^{+0.12}_{-0.12}$	$(8.81^{+0.65}_{-0.60}) \times 10^{52}$
6504	$154.8^{+4.0}_{-4.0}$	$1.67^{+0.07}_{-0.07}$	$(4.00^{+0.44}_{-0.41}) \times 10^{52}$
6521	$133.4^{+24.3}_{-25.7}$	$7.15^{+8.07}_{-3.39}$	$(2.78^{+12.59}_{-2.16}) \times 10^{53}$
6522	$98.1^{+21.4}_{-83.0}$	$1.47^{+0.59}_{-1.31}$	$(1.38^{+1.76}_{-1.37}) \times 10^{52}$
6523	$92.4^{+58.6}_{-27.5}$	$1.48^{+2.40}_{-0.59}$	$(1.23^{+11.51}_{-0.88}) \times 10^{52}$
6525	$349.9^{+25.2}_{-36.6}$	$10.19^{+4.18}_{-3.60}$	$(3.60^{+4.21}_{-2.27}) \times 10^{54}$
6528	$222.4^{+16.1}_{-15.3}$	$7.83^{+2.66}_{-1.76}$	$(9.04^{+8.56}_{-4.01}) \times 10^{53}$
6531	$66.2^{+4.7}_{-5.0}$	$3.13^{+0.55}_{-0.49}$	$(1.76^{+0.83}_{-0.59}) \times 10^{52}$
6538	$48.6^{+6.9}_{-10.1}$	$0.83^{+0.16}_{-0.21}$	$(1.86^{+1.01}_{-0.94}) \times 10^{51}$
6539	$310.4^{+64.2}_{-76.9}$	$4.10^{+3.26}_{-1.92}$	$(5.89^{+17.14}_{-4.59}) \times 10^{53}$

TABLE 2—*Continued*

Trigger Number	E_p (keV)	Redshift	Luminosity (ergs s^{-1})
6546	$73.6^{+3.6}_{-3.6}$	$1.55^{+0.13}_{-0.12}$	$(8.30^{+1.75}_{-1.48}) \times 10^{51}$
6552	$36.7^{+15.0}_{-22.8}$	$1.05^{+0.73}_{-0.72}$	$(1.32^{+3.50}_{-1.25}) \times 10^{51}$
6554	$69.3^{+10.8}_{-9.8}$	$1.71^{+0.50}_{-0.37}$	$(8.26^{+7.24}_{-3.72}) \times 10^{51}$
6560	$177.9^{+4.0}_{-3.9}$	$2.46^{+0.11}_{-0.11}$	$(8.89^{+1.02}_{-0.90}) \times 10^{52}$
6564	$117.0^{+21.3}_{-17.5}$	$5.79^{+5.26}_{-2.12}$	$(1.48^{+5.04}_{-0.98}) \times 10^{53}$
6578	$107.2^{+54.3}_{-60.7}$	$3.77^{+14.34}_{-2.88}$	$(6.12^{+217.26}_{-5.94}) \times 10^{52}$
6582	$69.6^{+53.9}_{-47.9}$	$1.72^{+4.83}_{-1.35}$	$(8.42^{+195.73}_{-8.21}) \times 10^{51}$
6583	$90.4^{+4.9}_{-4.2}$	$6.67^{+1.45}_{-0.98}$	$(1.13^{+0.64}_{-0.35}) \times 10^{53}$
6585	$48.2^{+41.4}_{-28.4}$	$0.81^{+1.25}_{-0.52}$	$(1.78^{+15.83}_{-1.63}) \times 10^{51}$
6587	$326.5^{+4.4}_{-4.6}$	$1.07^{+0.02}_{-0.02}$	$(1.07^{+0.05}_{-0.05}) \times 10^{53}$
6593	$261.4^{+5.7}_{-5.6}$	$2.40^{+0.11}_{-0.10}$	$(1.86^{+0.20}_{-0.18}) \times 10^{53}$
6598	$73.2^{+24.2}_{-8.6}$	$1.90^{+1.50}_{-0.36}$	$(1.06^{+3.25}_{-0.42}) \times 10^{52}$
6601	$39.3^{+49.2}_{-22.5}$	$0.82^{+2.28}_{-0.52}$	$(1.20^{+29.77}_{-1.09}) \times 10^{51}$
6605	$117.9^{+8.9}_{-8.6}$	$2.86^{+0.51}_{-0.42}$	$(4.86^{+2.35}_{-1.54}) \times 10^{52}$
6610	$72.4^{+5.5}_{-4.4}$	$1.95^{+0.28}_{-0.20}$	$(1.07^{+0.42}_{-0.25}) \times 10^{52}$
6611	$112.3^{+43.5}_{-25.8}$	$3.50^{+6.53}_{-1.47}$	$(5.98^{+63.28}_{-4.37}) \times 10^{52}$
6621	$115.4^{+13.2}_{-10.9}$	$0.97^{+0.16}_{-0.12}$	$(1.22^{+0.55}_{-0.34}) \times 10^{52}$
6625	$81.7^{+7.9}_{-7.4}$	$2.18^{+0.43}_{-0.34}$	$(1.58^{+0.88}_{-0.54}) \times 10^{52}$
6629	$419.2^{+95.7}_{-77.4}$	$8.69^{+18.91}_{-4.29}$	$(3.87^{+47.02}_{-3.07}) \times 10^{54}$
6630	$288.4^{+5.3}_{-5.2}$	$1.90^{+0.06}_{-0.06}$	$(1.65^{+0.14}_{-0.12}) \times 10^{53}$
6631	$92.7^{+35.2}_{-33.5}$	$2.74^{+3.71}_{-1.49}$	$(2.83^{+18.48}_{-2.41}) \times 10^{52}$
6641	$42.5^{+42.0}_{-21.3}$	$0.91^{+1.89}_{-0.52}$	$(1.55^{+22.67}_{-1.34}) \times 10^{51}$
6649	$87.1^{+21.9}_{-33.8}$	$6.65^{+12.29}_{-4.64}$	$(1.04^{+10.03}_{-0.98}) \times 10^{53}$
6657	$93.8^{+34.2}_{-41.7}$	$3.03^{+4.28}_{-1.93}$	$(3.36^{+23.20}_{-3.07}) \times 10^{52}$
6666	$88.5^{+42.0}_{-49.0}$	$4.82^{+25.14}_{-3.78}$	$(6.23^{+377.00}_{-6.08}) \times 10^{52}$
6672	$116.2^{+15.9}_{-15.4}$	$1.35^{+0.31}_{-0.26}$	$(1.75^{+1.14}_{-0.71}) \times 10^{52}$
6683	$188.3^{+15.7}_{-14.9}$	$5.40^{+1.65}_{-1.14}$	$(3.41^{+2.92}_{-1.46}) \times 10^{53}$
6762	$129.6^{+36.7}_{-39.0}$	$6.31^{+13.92}_{-3.80}$	$(2.11^{+27.16}_{-1.87}) \times 10^{53}$
6763	$155.0^{+32.4}_{-21.2}$	$3.54^{+2.50}_{-0.99}$	$(1.16^{+2.92}_{-0.63}) \times 10^{53}$
6767	$88.9^{+32.7}_{-46.3}$	$3.86^{+7.40}_{-2.83}$	$(4.38^{+47.81}_{-4.21}) \times 10^{52}$
6802	$123.1^{+36.1}_{-40.8}$	$3.60^{+4.26}_{-1.97}$	$(7.51^{+39.12}_{-6.42}) \times 10^{52}$
6814	$197.6^{+28.0}_{-23.8}$	$4.19^{+2.03}_{-1.13}$	$(2.47^{+3.76}_{-1.30}) \times 10^{53}$
6816	$85.3^{+3.5}_{-6.9}$	$0.87^{+0.05}_{-0.09}$	$(5.97^{+0.84}_{-1.39}) \times 10^{51}$
6830	$93.6^{+28.0}_{-18.1}$	$7.36^{+23.36}_{-3.53}$	$(1.43^{+33.44}_{-1.12}) \times 10^{53}$
6877	$143.8^{+11.2}_{-12.6}$	$7.44^{+2.66}_{-1.99}$	$(3.46^{+3.48}_{-1.78}) \times 10^{53}$
6882	$44.7^{+35.8}_{-50.1}$	$1.14^{+2.09}_{-1.04}$	$(2.15^{+25.10}_{-2.14}) \times 10^{51}$
6892	$196.8^{+58.0}_{-61.2}$	$5.42^{+10.52}_{-3.19}$	$(3.74^{+39.94}_{-3.30}) \times 10^{53}$
6904	$1206.0^{+32.8}_{-31.5}$	$4.14^{+0.31}_{-0.28}$	$(9.03^{+1.69}_{-1.36}) \times 10^{54}$
6917	$153.0^{+27.7}_{-29.3}$	$2.27^{+0.95}_{-0.71}$	$(5.86^{+7.77}_{-3.51}) \times 10^{52}$
6930	$100.4^{+7.4}_{-6.9}$	$1.02^{+0.11}_{-0.09}$	$(9.70^{+2.72}_{-2.04}) \times 10^{51}$
6963	$199.3^{+36.8}_{-29.7}$	$1.05^{+0.29}_{-0.20}$	$(3.91^{+3.27}_{-1.61}) \times 10^{52}$
7012	$300.4^{+5.1}_{-4.9}$	$1.64^{+0.05}_{-0.04}$	$(1.48^{+0.10}_{-0.10}) \times 10^{53}$
7028	$208.2^{+20.7}_{-17.8}$	$1.07^{+0.16}_{-0.12}$	$(4.38^{+1.74}_{-1.14}) \times 10^{52}$
7030	$52.2^{+29.4}_{-23.8}$	$1.25^{+1.48}_{-0.69}$	$(3.24^{+18.51}_{-2.78}) \times 10^{51}$
7087	$197.3^{+57.4}_{-48.7}$	$7.14^{+20.09}_{-3.96}$	$(6.05^{+115.22}_{-5.14}) \times 10^{53}$
7207	$136.8^{+41.7}_{-31.0}$	$7.23^{+23.49}_{-3.82}$	$(2.98^{+72.29}_{-2.47}) \times 10^{53}$
7209	$81.9^{+37.1}_{-13.7}$	$1.56^{+1.61}_{-0.38}$	$(1.03^{+4.74}_{-0.51}) \times 10^{52}$
7213	$72.5^{+19.3}_{-31.4}$	$3.60^{+3.68}_{-2.35}$	$(2.61^{+10.95}_{-2.41}) \times 10^{52}$
7228	$175.8^{+26.8}_{-21.6}$	$3.22^{+1.40}_{-0.79}$	$(1.29^{+1.75}_{-0.63}) \times 10^{53}$
7230	$190.1^{+37.4}_{-27.8}$	$10.08^{+19.57}_{-4.49}$	$(1.04^{+10.37}_{-0.77}) \times 10^{54}$
7240	$612.0^{+101.8}_{-98.1}$	$11.48^{+18.71}_{-5.68}$	$(1.37^{+10.26}_{-1.08}) \times 10^{55}$
7250	$134.6^{+12.3}_{-11.1}$	$3.30^{+0.80}_{-0.57}$	$(7.85^{+5.33}_{-2.88}) \times 10^{52}$
7255	$240.5^{+23.5}_{-21.8}$	$3.98^{+1.19}_{-0.82}$	$(3.37^{+2.85}_{-1.43}) \times 10^{53}$
7263	$41.9^{+54.3}_{-31.6}$	$0.81^{+2.34}_{-0.64}$	$(1.34^{+36.03}_{-1.31}) \times 10^{51}$
7285	$93.1^{+36.7}_{-33.9}$	$2.05^{+2.20}_{-1.04}$	$(1.89^{+9.02}_{-1.56}) \times 10^{52}$
7293	$186.5^{+17.9}_{-16.1}$	$8.48^{+4.35}_{-2.38}$	$(7.33^{+11.42}_{-3.89}) \times 10^{53}$
7295	$353.4^{+16.9}_{-15.7}$	$5.65^{+0.95}_{-0.73}$	$(1.30^{+0.56}_{-0.36}) \times 10^{54}$
7298	$141.4^{+42.7}_{-15.1}$	$7.35^{+23.97}_{-2.29}$	$(3.27^{+79.81}_{-1.90}) \times 10^{53}$
7301	$564.8^{+10.6}_{-10.3}$	$1.10^{+0.03}_{-0.03}$	$(3.31^{+0.23}_{-0.20}) \times 10^{53}$
7319	$164.9^{+37.4}_{-26.6}$	$5.75^{+7.39}_{-2.22}$	$(2.91^{+16.29}_{-1.98}) \times 10^{53}$
7323	$96.4^{+40.1}_{-43.2}$	$5.42^{+24.31}_{-3.91}$	$(8.99^{+404.36}_{-8.57}) \times 10^{52}$
7328	$103.4^{+28.1}_{-10.9}$	$6.92^{+15.93}_{-2.08}$	$(1.57^{+21.53}_{-0.89}) \times 10^{53}$
7374	$193.4^{+8.3}_{-6.8}$	$2.90^{+0.28}_{-0.21}$	$(1.34^{+0.34}_{-0.22}) \times 10^{53}$
7390	$254.4^{+18.8}_{-17.1}$	$11.28^{+5.17}_{-2.95}$	$(2.29^{+3.04}_{-1.14}) \times 10^{54}$
7403	$144.8^{+25.7}_{-22.6}$	$10.02^{+15.75}_{-4.65}$	$(5.98^{+42.94}_{-4.56}) \times 10^{53}$

TABLE 2—*Continued*

Trigger Number	E_p (keV)	Redshift	Luminosity (ergs s^{-1})
7429	$223.5^{+9.2}_{-8.7}$	$9.50^{+1.91}_{-1.43}$	$(1.29^{+0.66}_{-0.40}) \times 10^{54}$
7446	$138.8^{+15.3}_{-14.4}$	$1.40^{+0.26}_{-0.21}$	$(2.60^{+1.32}_{-0.86}) \times 10^{52}$
7452	$90.8^{+21.2}_{-167.4}$	$4.14^{+3.95}_{-1.38}$	$(5.10^{+19.22}_{-3.16}) \times 10^{52}$
7464	$367.2^{+92.9}_{-126.1}$	$6.61^{+12.29}_{-4.33}$	$(1.83^{+17.84}_{-1.69}) \times 10^{54}$
7469	$67.5^{+39.6}_{-24.6}$	$1.08^{+1.20}_{-0.48}$	$(4.63^{+24.34}_{-3.52}) \times 10^{51}$
7475	$149.4^{+14.9}_{-13.1}$	$1.93^{+0.37}_{-0.28}$	$(4.50^{+2.41}_{-1.44}) \times 10^{52}$
7477	$232.2^{+35.5}_{-29.7}$	$5.65^{+3.90}_{-1.81}$	$(5.59^{+13.10}_{-3.34}) \times 10^{53}$
7481	$114.9^{+32.3}_{-54.5}$	$3.59^{+3.98}_{-2.47}$	$(6.53^{+30.82}_{-6.14}) \times 10^{52}$
7487	$79.2^{+7.4}_{-7.0}$	$2.34^{+0.47}_{-0.37}$	$(1.64^{+0.91}_{-0.56}) \times 10^{52}$
7491	$428.6^{+6.1}_{-6.0}$	$2.03^{+0.05}_{-0.05}$	$(3.94^{+0.26}_{-0.24}) \times 10^{53}$
7494	$111.0^{+16.1}_{-14.9}$	$4.69^{+2.57}_{-1.45}$	$(9.36^{+16.51}_{-5.46}) \times 10^{52}$
7497	$133.0^{+16.0}_{-19.7}$	$5.76^{+2.92}_{-2.09}$	$(1.89^{+2.98}_{-1.24}) \times 10^{53}$
7502	$110.2^{+47.0}_{-41.3}$	$3.69^{+9.00}_{-2.21}$	$(6.26^{+102.51}_{-5.57}) \times 10^{52}$
7503	$198.2^{+13.5}_{-12.8}$	$3.68^{+0.69}_{-0.54}$	$(2.02^{+1.01}_{-0.64}) \times 10^{53}$
7504	$116.6^{+21.9}_{-22.4}$	$4.07^{+2.80}_{-1.57}$	$(8.20^{+19.72}_{-5.65}) \times 10^{52}$
7515	$221.2^{+13.0}_{-12.0}$	$5.44^{+1.12}_{-0.83}$	$(4.76^{+2.61}_{-1.53}) \times 10^{53}$
7527	$400.7^{+9.9}_{-9.6}$	$3.80^{+0.25}_{-0.22}$	$(8.69^{+1.39}_{-1.16}) \times 10^{53}$
7528	$70.7^{+31.2}_{-45.8}$	$2.61^{+4.33}_{-2.05}$	$(1.53^{+13.85}_{-1.49}) \times 10^{52}$
7529	$177.8^{+11.5}_{-10.6}$	$2.38^{+0.32}_{-0.26}$	$(8.47^{+3.05}_{-2.10}) \times 10^{52}$
7530	$146.9^{+6.4}_{-6.2}$	$1.28^{+0.09}_{-0.08}$	$(2.63^{+0.45}_{-0.38}) \times 10^{52}$
7548	$184.2^{+21.2}_{-17.6}$	$5.57^{+2.59}_{-1.40}$	$(3.44^{+4.87}_{-1.70}) \times 10^{53}$
7550	$120.4^{+21.6}_{-16.1}$	$2.03^{+0.78}_{-0.44}$	$(3.12^{+3.76}_{-1.42}) \times 10^{52}$
7551	$71.1^{+35.0}_{-14.7}$	$2.08^{+3.20}_{-0.67}$	$(1.12^{+9.29}_{-0.69}) \times 10^{52}$
7564	$82.1^{+3.4}_{-5.7}$	$2.10^{+0.16}_{-0.25}$	$(1.53^{+0.31}_{-0.41}) \times 10^{52}$
7566	$40.7^{+8.6}_{-11.1}$	$1.07^{+0.35}_{-0.37}$	$(1.66^{+1.66}_{-1.07}) \times 10^{51}$
7567	$68.9^{+5.3}_{-5.8}$	$1.82^{+0.25}_{-0.25}$	$(8.84^{+3.33}_{-2.66}) \times 10^{51}$
7568	$49.4^{+25.8}_{-25.6}$	$1.84^{+2.74}_{-1.19}$	$(4.61^{+36.68}_{-4.25}) \times 10^{51}$
7573	$52.2^{+16.2}_{-23.8}$	$0.96^{+0.46}_{-0.51}$	$(2.45^{+3.96}_{-2.05}) \times 10^{51}$
7575	$467.9^{+6.2}_{-6.1}$	$2.82^{+0.08}_{-0.08}$	$(7.51^{+0.54}_{-0.50}) \times 10^{53}$
7579	$31.3^{+32.8}_{-25.3}$	$0.74^{+1.40}_{-0.62}$	$(6.94^{+87.92}_{-6.83}) \times 10^{50}$
7588	$74.7^{+2.6}_{-11.5}$	$1.44^{+0.08}_{-0.32}$	$(7.79^{+1.12}_{-3.57}) \times 10^{51}$
7598	$109.3^{+15.6}_{-15.0}$	$2.34^{+0.75}_{-0.55}$	$(3.12^{+2.99}_{-1.50}) \times 10^{52}$
7603	$93.6^{+20.2}_{-39.2}$	$2.31^{+1.21}_{-1.33}$	$(2.24^{+3.94}_{-1.97}) \times 10^{52}$
7605	$136.2^{+27.1}_{-17.3}$	$4.06^{+3.02}_{-1.13}$	$(1.12^{+2.97}_{-0.60}) \times 10^{53}$
7607	$60.9^{+4.0}_{-5.0}$	$0.95^{+0.09}_{-0.10}$	$(3.29^{+0.79}_{-0.80}) \times 10^{51}$
7608	$92.4^{+23.9}_{-20.1}$	$7.33^{+16.46}_{-3.79}$	$(1.39^{+18.13}_{-1.14}) \times 10^{53}$
7630	$127.2^{+24.2}_{-31.1}$	$4.09^{+2.88}_{-1.89}$	$(9.85^{+24.37}_{-7.63}) \times 10^{52}$
7638	$66.8^{+3.3}_{-3.3}$	$1.74^{+0.15}_{-0.14}$	$(7.83^{+1.79}_{-1.45}) \times 10^{51}$
7645	$70.7^{+15.9}_{-25.8}$	$2.54^{+1.51}_{-1.36}$	$(1.47^{+3.01}_{-1.24}) \times 10^{52}$
7657	$74.7^{+2.7}_{-2.9}$	$1.03^{+0.05}_{-0.05}$	$(5.41^{+0.70}_{-0.67}) \times 10^{51}$
7677	$73.4^{+7.3}_{-17.7}$	$2.07^{+0.41}_{-0.76}$	$(1.19^{+0.66}_{-0.80}) \times 10^{52}$
7678	$323.5^{+7.4}_{-7.2}$	$2.96^{+0.15}_{-0.14}$	$(3.86^{+0.50}_{-0.43}) \times 10^{53}$
7688	$258.0^{+30.9}_{-27.6}$	$5.73^{+2.87}_{-1.60}$	$(7.07^{+10.98}_{-3.80}) \times 10^{53}$
7695	$871.4^{+42.4}_{-39.8}$	$6.32^{+1.17}_{-0.89}$	$(9.56^{+4.57}_{-2.84}) \times 10^{54}$
7701	$185.3^{+33.6}_{-29.8}$	$9.09^{+13.18}_{-4.16}$	$(8.20^{+52.62}_{-6.20}) \times 10^{53}$
7703	$174.6^{+81.4}_{-54.4}$	$3.82^{+12.03}_{-2.04}$	$(1.66^{+41.97}_{-1.40}) \times 10^{53}$
7705	$44.3^{+59.0}_{-31.1}$	$0.98^{+3.72}_{-0.74}$	$(1.80^{+79.57}_{-1.74}) \times 10^{51}$
7707	$62.8^{+37.2}_{-34.2}$	$2.87^{+9.96}_{-2.06}$	$(1.39^{+43.50}_{-1.33}) \times 10^{52}$
7711	$206.6^{+11.4}_{-10.9}$	$5.15^{+0.96}_{-0.74}$	$(3.79^{+1.85}_{-1.16}) \times 10^{53}$
7727	$126.6^{+12.3}_{-14.4}$	$4.00^{+1.18}_{-1.00}$	$(9.40^{+7.91}_{-4.69}) \times 10^{52}$
7744	$79.5^{+2.4}_{-2.7}$	$1.85^{+0.10}_{-0.11}$	$(1.20^{+0.16}_{-0.16}) \times 10^{52}$
7750	$90.9^{+74.0}_{-37.4}$	$2.08^{+8.90}_{-1.16}$	$(1.84^{+89.71}_{-1.59}) \times 10^{52}$
7762	$103.9^{+16.3}_{-30.3}$	$2.83^{+1.17}_{-1.33}$	$(3.72^{+4.76}_{-2.93}) \times 10^{52}$
7769	$120.1^{+43.8}_{-31.4}$	$3.33^{+5.23}_{-1.51}$	$(6.34^{+51.18}_{-4.87}) \times 10^{52}$
7770	$121.9^{+51.1}_{-37.6}$	$2.48^{+3.53}_{-1.16}$	$(4.21^{+30.22}_{-3.32}) \times 10^{52}$
7781	$121.2^{+12.4}_{-11.3}$	$1.76^{+0.33}_{-0.26}$	$(2.61^{+1.36}_{-0.85}) \times 10^{52}$
7785	$148.3^{+8.8}_{-4.3}$	$4.24^{+0.75}_{-0.31}$	$(1.41^{+0.66}_{-0.24}) \times 10^{53}$
7786	$101.9^{+31.4}_{-49.8}$	$1.19^{+0.63}_{-0.69}$	$(1.17^{+2.14}_{-1.02}) \times 10^{52}$
7788	$244.4^{+28.4}_{-31.8}$	$10.08^{+7.86}_{-4.15}$	$(1.72^{+4.54}_{-1.21}) \times 10^{54}$
7803	$97.5^{+7.0}_{-6.7}$	$2.98^{+0.52}_{-0.42}$	$(3.54^{+1.64}_{-1.08}) \times 10^{52}$
7818	$178.8^{+38.9}_{-52.0}$	$8.79^{+17.56}_{-5.66}$	$(7.19^{+76.01}_{-6.55}) \times 10^{53}$
7822	$96.7^{+10.8}_{-10.4}$	$1.57^{+0.31}_{-0.26}$	$(1.44^{+0.79}_{-0.51}) \times 10^{52}$
7831	$92.3^{+43.7}_{-44.1}$	$3.03^{+6.94}_{-2.03}$	$(3.26^{+49.05}_{-3.04}) \times 10^{52}$
7840	$172.1^{+8.5}_{-8.1}$	$6.56^{+1.26}_{-0.97}$	$(3.97^{+1.98}_{-1.23}) \times 10^{53}$
7841	$109.2^{+56.8}_{-49.1}$	$2.38^{+4.74}_{-1.46}$	$(3.20^{+39.51}_{-2.89}) \times 10^{52}$

TABLE 2—*Continued*

Trigger Number	E_p (keV)	Redshift	Luminosity (ergs s^{-1})
7845	$448.6^{+103.4}_{-92.8}$	$10.90^{+34.18}_{-6.18}$	$(6.68^{+145.13}_{-5.71}) \times 10^{54}$
7858	$96.4^{+2.5}_{-2.6}$	$1.67^{+0.07}_{-0.07}$	$(1.55^{+0.17}_{-0.16}) \times 10^{52}$
7868	$214.8^{+56.9}_{-32.1}$	$8.98^{+29.20}_{-3.89}$	$(1.08^{+25.51}_{-0.79}) \times 10^{54}$
7886	$126.8^{+7.1}_{-62.1}$	$4.45^{+0.75}_{-3.24}$	$(1.12^{+0.50}_{-1.07}) \times 10^{53}$
7929	$684.4^{+83.7}_{-70.9}$	$9.94^{+8.28}_{-3.45}$	$(1.32^{+3.80}_{-0.82}) \times 10^{55}$
7932	$140.8^{+20.4}_{-16.2}$	$3.51^{+1.53}_{-0.84}$	$(9.47^{+12.78}_{-4.56}) \times 10^{52}$
7934	$45.4^{+40.8}_{-39.5}$	$1.42^{+4.10}_{-1.29}$	$(2.82^{+71.22}_{-2.81}) \times 10^{51}$
7938	$149.1^{+38.8}_{-30.3}$	$8.51^{+24.17}_{-4.43}$	$(4.72^{+89.27}_{-3.86}) \times 10^{53}$
7954	$244.2^{+5.4}_{-5.3}$	$0.97^{+0.03}_{-0.03}$	$(5.41^{+0.41}_{-0.38}) \times 10^{52}$
7969	$83.2^{+11.5}_{-6.1}$	$1.36^{+0.31}_{-0.15}$	$(9.00^{+5.92}_{-2.19}) \times 10^{51}$
7976	$171.6^{+2.4}_{-2.0}$	$2.35^{+0.07}_{-0.05}$	$(7.75^{+0.54}_{-0.41}) \times 10^{52}$
7987	$292.0^{+20.0}_{-17.8}$	$2.80^{+0.44}_{-0.34}$	$(2.88^{+1.23}_{-0.78}) \times 10^{53}$
7992	$23.0^{+33.4}_{-3.3}$	$0.60^{+1.57}_{-0.10}$	$(3.18^{+71.91}_{-1.12}) \times 10^{50}$
7994	$274.0^{+5.6}_{-5.5}$	$7.38^{+0.59}_{-0.52}$	$(1.24^{+0.24}_{-0.19}) \times 10^{54}$
7998	$90.6^{+2.3}_{-3.1}$	$1.42^{+0.06}_{-0.07}$	$(1.13^{+0.11}_{-0.14}) \times 10^{52}$
8001	$136.1^{+6.6}_{-6.4}$	$8.21^{+1.81}_{-1.36}$	$(3.69^{+2.11}_{-1.26}) \times 10^{53}$
8004	$74.9^{+24.0}_{-13.3}$	$0.99^{+0.50}_{-0.22}$	$(5.22^{+9.02}_{-2.44}) \times 10^{51}$
8008	$529.5^{+9.3}_{-9.1}$	$5.86^{+0.35}_{-0.32}$	$(3.09^{+0.44}_{-0.37}) \times 10^{54}$
8012	$93.9^{+46.2}_{-48.3}$	$3.84^{+14.01}_{-2.80}$	$(4.85^{+158.89}_{-4.65}) \times 10^{52}$
8019	$95.9^{+3.6}_{-3.5}$	$1.62^{+0.10}_{-0.10}$	$(1.48^{+0.24}_{-0.21}) \times 10^{52}$
8022	$136.0^{+25.3}_{-23.8}$	$1.70^{+0.61}_{-0.44}$	$(3.15^{+3.51}_{-1.65}) \times 10^{52}$
8026	$70.0^{+34.1}_{-41.3}$	$3.03^{+7.38}_{-2.30}$	$(1.87^{+31.24}_{-1.81}) \times 10^{52}$
8030	$166.7^{+13.7}_{-13.1}$	$3.14^{+0.65}_{-0.51}$	$(1.12^{+0.64}_{-0.39}) \times 10^{53}$
8036	$106.7^{+4.9}_{-4.8}$	$3.65^{+0.44}_{-0.38}$	$(5.79^{+1.80}_{-1.35}) \times 10^{52}$
8049	$23.3^{+45.6}_{-15.4}$	$0.46^{+1.55}_{-0.31}$	$(2.70^{+97.79}_{-2.51}) \times 10^{50}$
8050	$81.7^{+3.2}_{-3.2}$	$1.49^{+0.10}_{-0.09}$	$(9.74^{+1.61}_{-1.38}) \times 10^{51}$
8059	$62.7^{+39.2}_{-28.8}$	$1.25^{+1.72}_{-0.69}$	$(4.68^{+33.74}_{-4.02}) \times 10^{51}$
8063	$260.7^{+47.3}_{-43.4}$	$7.41^{+8.59}_{-3.22}$	$(1.13^{+5.30}_{-0.83}) \times 10^{54}$
8064	$61.9^{+5.0}_{-19.6}$	$2.36^{+0.41}_{-1.11}$	$(1.01^{+0.48}_{-0.80}) \times 10^{52}$
8066	$83.5^{+19.1}_{-63.4}$	$2.41^{+1.40}_{-2.06}$	$(1.90^{+3.82}_{-1.88}) \times 10^{52}$
8073	$127.5^{+80.3}_{-50.9}$	$2.14^{+5.37}_{-1.18}$	$(3.76^{+69.54}_{-3.23}) \times 10^{52}$
8075	$138.8^{+11.7}_{-10.8}$	$2.72^{+0.54}_{-0.41}$	$(6.26^{+3.38}_{-2.04}) \times 10^{52}$
8084	$126.0^{+4.9}_{-4.9}$	$6.15^{+0.88}_{-0.74}$	$(1.91^{+0.69}_{-0.49}) \times 10^{53}$
8087	$341.3^{+43.5}_{-38.5}$	$6.96^{+4.46}_{-2.21}$	$(1.73^{+3.63}_{-1.02}) \times 10^{54}$
8098	$148.6^{+19.3}_{-16.3}$	$2.06^{+0.55}_{-0.38}$	$(4.85^{+3.78}_{-1.90}) \times 10^{52}$
8099	$79.5^{+12.1}_{-11.3}$	$0.74^{+0.15}_{-0.13}$	$(4.49^{+2.54}_{-1.66}) \times 10^{51}$
8105	$17.1^{+5.5}_{-5.4}$	$0.41^{+0.15}_{-0.14}$	$(1.36^{+1.55}_{-0.84}) \times 10^{50}$
8111	$354.5^{+46.6}_{-88.3}$	$7.98^{+6.05}_{-4.60}$	$(2.38^{+6.15}_{-2.06}) \times 10^{54}$
8116	$241.2^{+30.7}_{-18.2}$	$11.78^{+12.32}_{-3.44}$	$(2.23^{+8.69}_{-1.21}) \times 10^{54}$
8121	$103.8^{+24.7}_{-20.9}$	$8.43^{+19.23}_{-4.34}$	$(2.25^{+29.58}_{-1.83}) \times 10^{53}$

NOTE.—Table 2 is also available in machine-readable form in the electronic edition of the *Astrophysical Journal*.

REFERENCES

Amati, L., et al. 2002, A&A, 390, 81
Andersen M. I., et al. 2000, A&A, 364, L54
Atteia, J. L. 2003, A&A, 407, L1
Band, D. L. 2003, ApJ, 588, 945
Band, D. L., et al. 1993, ApJ, 413, 281
Barger, A. J., Cowie, L. L., & Richards, E. A. 2000, AJ, 119, 2092
Bennett, C. L., et al. 2003, ApJS, 148, 1
Bloom, J. S., Frail, D. A., & Kulkarni, S. R. 2003, ApJ, 594, 674
Bloom, J. S., Frail, D. A., & Sari, R. 2001, AJ, 121, 2879
Caditz, D., & Petrosian, V. 1990, ApJ, 357, 326
Efron, B., & Petrosian, V. 1992, ApJ, 399, 345
Fenimore, E. E., & Ramirez-Ruiz, E. 2000, preprint (astro-ph/0004176)
Frail, D. A., et al. 2001, ApJ, 562, L55
Fryer, C. L., Woosley, S. E., & Hartmann, D. H. 1999, ApJ, 526, 152
Hjorth, J., et al. 2003, Nature, 423, 847
Ioka, K., & Nakamura, T. 2001, ApJ, 554, L163
Lilly, S. J., LeFevre, O., Hammer, F., & Crampton, D. 1996, ApJ, 460, L1
Lloyd-Ronning, N. M., Fryer, C. L., & Ramirez-Ruiz, E. 2002a, ApJ, 574, 554
———. 2002b, ApJ, 576, 101
Lynden-Bell, D. 1971, MNRAS, 155, 95
MacFadyen, A. I., & Woosley, S. E. 1999, ApJ, 524, 262
Madau, P., et al. 1996, MNRAS, 283, 1388
Maloney, A., & Petrosian, V. 1999, ApJ, 518, 32
Murakami, T., Yonetoku, D., Izawa, H., & Ioka, K. 2003, PASJ, 55, L65
Norris, J. P. 2002, ApJ, 579, 386
Norris, J. P., Marani, G. F., & Bonnell, J. T. 2000, ApJ, 534, 248
Petrosian, V. 1993, ApJ, 402, L33
Price, P. A., et al. 2003, Nature, 423, 844
Schaefer, B. E. 2003a, ApJ, 583, L67
———. 2003b, ApJ, 583, L71
Schaefer, B. E., Bradley, E., Deng, M., & Band, D. L. 2001, ApJ, 563, L123
Spergel, D. N., et al. 2003, ApJS, 148, 175
Stanek, K. Z., et al. 2003, ApJ, 591, L17
Stanway, E. R., Bunker, A. J., & McMahon, R. G. 2003, MNRAS, 342, 439
Uemura, M., et al. 2003, Nature, 423, 843
Wei, D. M. 2002, MNRAS, submitted (astro-ph/0212513)
Yamazaki, R., Ioka, K., & Nakamura, T. 2002, ApJ, 571, L31
Yamazaki, R., Yonetoku, D., & Nakamura, T. 2003, ApJ, 594, L79